Integrated Project - EUWB

Contract No 215669

Deliverable

D3.3.3

Application-aware algorithm and system design for multi-user enhancements for VHDR

Contractual data:	**M40**
Actual data:	**M40**
Authors:	**Henna Paaso, Markku Kiviranta, Antti Anttonen, Aarne Mammela, Emil Dimitrov, Sondos Alaa, Claus Kupferschmidt and Thomas Kaiser**
Participants:	**VTT, LUH**
Work package:	**WP3**
Security:	**PU**
Nature:	**Report**
Version:	**v1.0**
Total number of pages:	**42**

Abstract

This deliverable presents a study of some selected potential signal processing approaches to mitigate multiuser interference in UWB channels. Specifically, we investigate alternative mitigation methods including beamforming, time-reversal and detect-and-avoid techniques and evaluate the corresponding error performance in specific UWB channel environments.

Keywords

Beamforming, ultra-wideband, orthogonal frequency division multiplexing, error probability, multiuser interference, detect-and-avoid, time reversal.

Table of Contents

List of Figures

List of Tables

Abbreviations

AOA	Angle-of-Arrival
BER	Bit Error Rate
CCI	Co-channel Interference
CM	Constant Modulus
CTI	Channel State Information
DAA	Detect-and-Avoid
EIRP	Effective Isotropic Radiation Power
HPBW	Half Power Beamwidth
HPA	High Power Amplification
LMS	Least Mean Squares
LNA	Low Noise Amplification
MAI	Multi Access Interference
MLM	Maximum Likelihood Method
MMSE	Minimum Mean Square Error
MB-OFDM	Multiband Orthogonal Frequency Division Multiplexing
MIMO	Multiple Input Multiple Output
MISO	Multiple Input Single Output
MV	Minimum Variance
MVDR	Minimum-variance Distortionless Response
MUI	Multi-user Interference
RLS	Recursive Least Squares
SIR	Signal-to-Interference Ratio
SLC	Sidelobe Canceller
SMI	Sample Matrix Inversion
SNIR	Signal-to-Noise-and-Interference Ratio
TR	Time Reversal
TRM	Transmit/Receive Module
ZF	Zero Forcing

1 Executive summary

This deliverable presents a study of some selected potential signal processing approaches to mitigate multiuser interference in ultra-wideband (UWB) channels. Specifically, we investigate alternative mitigation methods including beamforming (BM), detect-and-avoid (DAA), and time-reversal (TR) techniques. We then evaluate the corresponding error performances in specific UWB channel environments.

Regarding the beamforming approach, an extensive overview of existing approaches and their trade-off analysis is given first. We then focus on a specific recursive least squares method, which is found to be an appealing solution to estimate the beamforming weights for mitigating the multiuser interference in orthogonal frequency division multiplexing (OFDM) based UWB systems. Interesting study cases are identified with an emphasis to compare time- and frequency-domain beamforming approaches at the receiver. Extensive simulation study is conducted in the selected UWB channels with different interface scenarios, and it is found that the frequency-domain beamforming approach is more effective than the time-domain approach at the cost of increased complexity.

Time-reversal techniques combined with zero-forcing (ZF) beamforming are further applied in order to achieve maximum output signal-to-noise ratio (SNR) and reduce the multi-user interference (MUI) to victim devices and enhance the system reliability.

Finally, co-existence and interference testing results in the presence of WiMAX demonstrate the functionality of a flexible DAA approach based on spectrum sensing, band dropping or tone nulling to mitigate the harmful interference to victim systems. The performance of a flexible DAA algorithm is verified through measurements in the presence of WiMAX interference.

2 Introduction

In the foreseeable future, the large-scale deployment of ultra-wideband (UWB) wireless devices and the corresponding requirements of short-range communication applications, particularly those summarized in D3.1.1 [44], are expected to result in new challenges in terms of efficient exploitation of the achievable spectral resources. Major challenges include how to mitigate the interference caused by the desired signal itself as well as other users operating in the local environment.

MB-OFDM system has become the main signal transmission model for UWB communications. A main advantage of OFDM system is that the channel's delay spread becomes a significantly shorter fraction of a symbol period than in a single carrier serial system, thus mitigating the effect of self-interference. Regarding the multiuser interference, a vast amount of research contributions can be found on multiuser detection with OFDM and a good summary is found from [45]. On the other hand, beamforming (BM) and interference avoidance techniques with OFDM systems have been addressed only recently. Furthermore, an impulse radio (IR) system introduces many low complexity advantages over OFDM system. Interference mitigation with time-reversal (TR) techniques has been proposed as appealing solution in interference-limited systems [47]. However, there seems to be a need for further study to obtain insight how these techniques behave in dense UWB multipath fading channels. Consequently, our goal is to evaluate the potentiality of using BM and detect-and-avoid (DAA) interference avoidance to enhance the interference mitigation capabilities of the MB-OFDM system presented in [44]. Furthermore TR techniques are evaluated in different UWB channel environments for IR systems.

This report is organized as follows. The BM methods are first analysed in Section 3. An extensive overview of existing approaches and their trade-off analysis is given first, followed by a more detailed error analysis for selected methods. Section 4 presents the TR pre-filtering techniques with ZF beamforming. Finally, Section 5 provides a co-existence study and flexible DAA algorithm followed by the conclusions in Section 6.

3 Beamforming techniques

In this section, we investigate some promising beamforming techniques suitable for OFDM-based UWB communication systems. After an introduction to beamforming systems, we describe the system model of interest. Finally, the resulted error performance is studied in UWB indoor channels with different interference scenarios.

3.1 Preliminaries on beamforming systems

Beamforming can be realised by using antenna arrays. In general, the latter is a multi-input multi-output (MIMO) technique where multiple closely located antennas are employed either in the transmitter or in the receiver, or in both sides to direct more energy towards a desired direction in comparison with other directions. Multiple antennas allow the receiver to place a beam in the direction of the desired signal while nulling the interference. Beamforming also helps to reduce the power required for the information transmission because a narrow beam can be placed in a specific direction.

We discuss briefly the basic beamformer and its structure. The beamformers were first developed for narrowband signals that can be sufficiently characterized by a single frequency [3]. The general narrowband receiver beamformer structure is illustrated in Figure 3.1. In this beamformer, the signals from each antenna element are multiplied with complex weights and summed at the array output. Thus, the output of the beamformer becomes [33]

$$y(k) = \sum_{n=1}^{N} w_n x_n(k)$$

where w_n denote the weights of the beamformer and $x_n(k)$ is the input signal of the element.

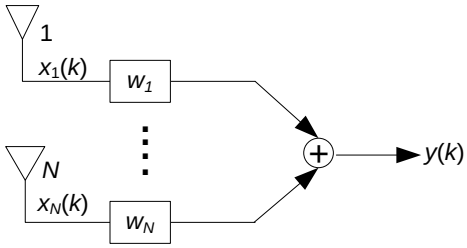

Figure 3.1. Illustration of a beamforming system.

For an ultra-wideband signal that has rich frequency content, such beamformers would not yield the same beam pattern for different frequencies. A common broadband beamformer is illustrated in Figure 3.2. The output of the beamformer in this case can be expressed as [33]

$$y(k) = \sum_{n=1}^{N} \sum_{p=0}^{K-1} w_{n,p} x_n(k-p)$$

where K is the number of delays at each of N antenna elements.

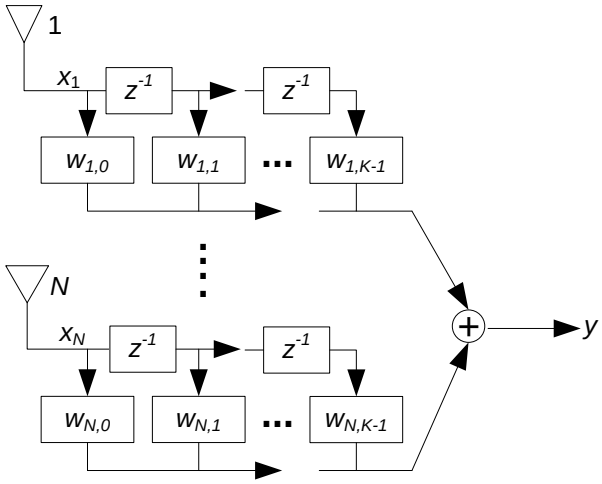

Figure 3.2. A common wideband beamforming system.

The basic idea of the beamforming is that different channels have to be correlated to each other. Compared to other MIMO techniques, such as diversity methods, therein the channels have to be uncorrelated. In the beamforming approach, antenna elements are spaced closely enough so that the Nyquist criterion for the spatial sampling is fulfilled. Therefore, transmitted or received signals add constructively for some directions and add destructively for some other directions. Furthermore, these directions can be adjusted by changing array weights. This effect is referred to as spatial filtering. So-called conventional beamformer steers the beam towards the desired signals, while null steering beamformers are designed in a way that the signal cancellation effect is maximized towards the undesired direction.

Adaptive beamformers iteratively control the directionality of a radiation pattern. Beamforming approaches can be divided into element-space and beam-space methods [28]. Element-space beamforming means that the data symbols are directly weighted with the array weights to form a beam. In beam-space beamforming, the data signal is processed by a multi-beam beamformer to form a suite of orthogonal beams and these beams are processed in beam-space. The criterion used for optimizing the weights is typically selected to be the minimum mean-squared error (MMSE), maximum signal-to-interference-and-noise ratio (SINR), or minimum-variance (MV) [28]. Furthermore, adaptive algorithms are commonly used for updating the weights. These algorithms include least mean squares (LMS), direct sample covariance matrix inversion, and recursive least squares (RLS). Another way to classify beamformers is to consider how the weights are chosen. In a data independent beamforming, the weights do not depend on the array data and are selected to present a specific response for all signal or interference scenarios. In a statistically optimum beamforming, the weights are chosen based on the statistics of the array data to optimize the array response. One efficient and simple way to produce scanning adaptive arrays is to use phase shifters at each radiating element [30]. Phased array beamforming is data independent. Three major types of RF phase shifters can be identified: 1) passive tuned, 2) switched delay lines, and 3) vector modulator. The vector modulator phase shifter is considered to be the most practical solution, especially with the CMOS implementation technology.

Steering and modifying an array beam pattern is a procedure enhancing the reception of the desired signal while simultaneously suppressing interfering signal through a complex weight selection [28].

An example of an adaptive beamforming system is shown in Figure 3.3. The choice of the weight parameters is based on the statistics of the signal vector $x(t)$ received at the array. The received signal y can be represented in matrix form

$$y = \begin{pmatrix} s_1 & \cdots & s_K \end{pmatrix} \begin{pmatrix} a_{11} & \cdots & a_{1N} \\ \vdots & \ddots & \vdots \\ a_{K1} & \cdots & a_{KN} \end{pmatrix} \begin{pmatrix} w_1 \\ \vdots \\ w_N \end{pmatrix}$$

where N is the number of the receiver antennas, s_k is the arrived signal (sources), K is number of the sources, and w_n is the nth beamforming weight. The array gain matrix is given as

$$\mathbf{a} = \begin{pmatrix} 1 & e^{j\frac{2\pi}{\lambda}d\sin\theta_1} & \cdots & e^{j\frac{2\pi}{\lambda}(N-1)d\sin\theta_1} \\ \vdots & \vdots & \ddots & \vdots \\ 1 & e^{j\frac{2\pi}{\lambda}d\sin\theta_K} & \cdots & e^{j\frac{2\pi}{\lambda}(N-1)d\sin\theta_K} \end{pmatrix}$$

and the steering vector for source 1 is

$$a_1 = \begin{pmatrix} 1 & e^{j\frac{2\pi}{\lambda}d\sin\theta_1} & \cdots & e^{j\frac{2\pi}{\lambda}(N-1)d\sin\theta_1} \end{pmatrix}.$$

The following example illustrates the system, which consists of two receiver (N = 2) antennas, one desired arrival signal, and one interfering signal (K = 2):

$$y = \begin{pmatrix} s_1 & s_2 \end{pmatrix} \begin{pmatrix} 1 & e^{j\frac{2\pi}{\lambda}d\sin\theta_1} \\ 1 & e^{j\frac{2\pi}{\lambda}d\sin\theta_2} \end{pmatrix} \begin{pmatrix} w_1 \\ w_2 \end{pmatrix},$$

where the desired signal is s_1 and the interfering signal is s_2. We can suppress the interference as

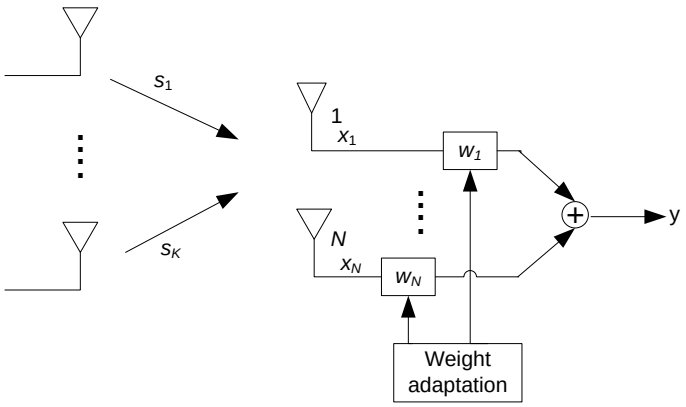

Figure 3.3. An adaptive beamforming system.

$$\begin{pmatrix} a_{11} & a_{12} \\ a_{21} & a_{22} \end{pmatrix}\begin{pmatrix} w_1 \\ w_2 \end{pmatrix} = \begin{pmatrix} w_1 + e^{j\frac{2\rho}{\prime}d\sin\theta_1} w_2 \\ w_1 + e^{j\frac{2\rho}{\prime}d\sin\theta_2} w_2 \end{pmatrix} = \begin{pmatrix} 1 \\ 0 \end{pmatrix}$$

$$\rightarrow \begin{cases} w_1 + e^{j\frac{2\pi}{\lambda}d\sin\theta_1} w_2 = 1 \\ w_1 + e^{j\frac{2\pi}{\lambda}d\sin\theta_2} w_2 = 0 \end{cases}.$$

We then solve w_1 and w_2 from these two last equations in order to cancel all interference and to retain the desired signal

$$y = \begin{bmatrix} s_1 & s_2 \end{bmatrix}\begin{pmatrix} 1 & e^{j\frac{2\pi}{\lambda}d\sin\theta_1} \\ 1 & e^{j\frac{2\pi}{\lambda}d\sin\theta_2} \end{pmatrix}\begin{pmatrix} w_1 \\ w_2 \end{pmatrix} = \begin{pmatrix} s_1 + s_2 & s_1 e^{j\frac{2\pi}{\lambda}d\sin\theta_1} + s_2 e^{j\frac{2\pi}{\lambda}d\sin\theta_2} \end{pmatrix}\begin{pmatrix} w_1 \\ w_2 \end{pmatrix}.$$

$$= (s_1 + s_2)w_1 + (s_1 e^{j\frac{2\pi}{\lambda}d\sin\theta_1} + s_2 e^{j\frac{2\pi}{\lambda}d\sin\theta_2})w_2 = \begin{bmatrix} s_1 & s_2 \end{bmatrix}\begin{pmatrix} 1 \\ 0 \end{pmatrix} = s1$$

The procedure in the above example exploits the fact that there is only one directional interference source and that it uses a priori information concerning the frequency and the directions of both of the signals [28]. However, a more practical processor should not require such detailed a priori information about the location, number, and nature of the signal sources.

In an adaptive beamforming, the maximum number of interferers that can be suppressed is upper-bounded by the number of antenna elements minus one (N-1) [34][38]. Thus, if we increase the size of the adaptive arrays, we can obtain better interference cancellation and also better resolution. As a result, two challenges are introduced including the required computational burden and the convergence speed for adaptation problems. Furthermore, the resulting high-resolution capability of using large arrays makes the array more sensitive to various imperfections.

Adaptive beamforming can be designed to be fully adaptive or only partially adaptive [28]. In fully adaptive beamforming, every available degree of freedom is used. This refers to the number of unconstrained or "free" weights that can be used to form a beam. Thus, every element or beam is individually adaptively controlled to achieve the maximum control of the beam pattern. Fully adaptive beamforming offers the following three advantages: 1) the full complements of the array's degrees of freedom are available to the beamformer, 2) the maximum aperture gain can be retained, because the entire array is employed, and 3) the maximum spatial resolution can be retained, because the entire array aperture is used. Fully adaptive beamforming may be difficult to implement in practice when the number of array elements becomes large. Thus, we can use a number of strategies for reducing the complexity. Only a fraction of the array elements for the adaptive control is judiciously selected, thus, adaptivity is carried out at the element level [29]. Alternatively, if all of the array elements can be grouped into subarrays, beamforming is carried out for each subarray, and the outputs of the subarray beamforming are adaptively controlled [7]. Finally, the entire array is used to form beams and these beams are steered in adaptive way [4]. The adaptive techniques require some sort of reference signals in their adaptive optimization process. The reference signal usually means explicit information about the signals of interest. Explicit reference can be divided in two parts including spatial reference and

temporal reference. Spatial reference is usually referred to as the angle-of-arrival (AOA) information of the desired signal. A temporal reference signal may be a pilot signal that is correlated with the desired signal. The used reference signal depends on the particular where adaptive beamforming is to be implemented.

Next, we briefly discuss some general performance characteristics for the beamforming. If the antenna element spacing *d* is too large compared to the wavelength λ, a second main lobe can appear in the radiation pattern [30]. The extra main lobes are referred to as grating lobes. To prevent a second main lobe, the spacing *d* has to be chosen according to the following criteria:

$$\frac{d}{\lambda} < \frac{1}{1+|\sin\theta_o|},$$

where θ_o denotes the AOA. The element spacing criteria depends on the desired main lobe direction. If the lobe is scanned close to the endfire ($\theta_o = \pm 90°$), the spacing has to be one half-wavelength apart to prevent grating lobes. The maximum spacing is 0.67λ when the desired direction is 30°. Figure 3.4 shows a grating lobe appearing when the spacing of the 8-element array is changed from 0.5λ to 0.9λ.

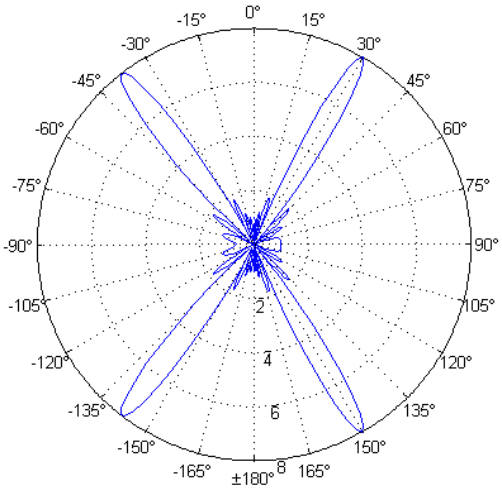

Figure 3.4. Array factor when the antenna elements are spaced 0.9 wavelengths apart.

Next, we clarify why the beamwidth becomes sharper when the number of elements increases. A useful measure of the sharpness of the array is the array directivity, which is defined as the ratio of the power radiated by an array in a particular desired direction to the average of the power radiated by the array in all directions [11]. The directivity can be presented as [30]

$$D_{\mathrm{e}} = \frac{|E(\theta_0)|^2}{|E(\theta)|^2_{average}}$$

where $|E(q)|^2_{average}$ is equal to the average of $|E(q)|^2$ and $E(q)$ is the radiated electric field that includes the effects of the element pattern and the array factor. The directivity of a uniformly weighted linear array of *N* isotropic radiators spaced $\lambda/2$ apart is equal to *N* independent of the main beam scan angle θ_0. There is no simple formula for determining the directivity of an array of nonisotrobic elements, as one must know the current distributions in each radiating element.

A 3-dB beamwidth, or half-power beamwidth (HPBW) for a linear array with uniform weighting can be defined as [28]

$$HPBW = \frac{0.88\lambda}{A}$$

where *A* is the aperture length of the array, which equals *Nd*. Thus, we can easily see that if the length of the array increases, the beamwidth becomes narrower.

In a multiuser communication system, there can be a relatively large number of co-channel interfering signals in comparison with the number of antenna elements. An exact analytical evaluation of the performance is quite complicated, for example when each of these interfering signals has a random amplitude due to channel fading. Analysis can be simplified so that only the strongest interferers are individually considered. The rest is considered as a lumped interference that is uncorrelated between elements. In [Litva96], it is shown that BER can be exhibit the following relationship:

$$BER \propto \frac{1}{(N\Gamma_1)^{N-1}}$$

where $N\Gamma_1$ is total interference-to-noise. Thus, the improvement in BER is mostly dependent on Γ_1 and *N*. Some studies have been carried out to investigate the effect of imperfect channel state information on the error performance. In [9], a transmit beamforming method for an OFDM system with limited feedback and beamformer interpolation is proposed. Limited feedback is also studied in [26]. This paper presents an interpolation technique for re-constructing of downsampled beamforming matrices in the frequency domain, and it also contains a useful list of references where efficient feedback schemes were reported.

3.2 Beamforming in OFDM systems

In this section, we describe in a more detail beamforming techniques optimized for OFDM systems whose error performance will be evaluated in the next section in selected UWB indoor channels. The beamforming techniques for OFDM systems can be divided into pre-FFT and post-FFT techniques at the receiver and post-IFFT and pre-IFFT techniques at the transmitter. Block diagrams of the OFDM receivers using pre-FFT and post-FFT are illustrated in Figure 3.5 and Figure 3.6. The array processing is applied in the time domain using pre-FFT and post-IFFT techniques, and in the frequency domain in the post-FFT and pre-IFFT parts of the system. The received signal is presented in the time domain as

$$\mathbf{V}(n) = \mathbf{A}(\theta)\mathbf{X}_L(n) + \mathbf{N}(n)$$

where

$$\mathbf{V}(n)=\begin{bmatrix} v_1(n,0) & v_1(n,1) & \cdots & v_1(n,K-1) \\ v_2(n,0) & v_2(n,1) & \cdots & v_2(n,K-1) \\ \vdots & \vdots & \ddots & \vdots \\ v_N(n,0) & v_N(n,1) & \cdots & v_N(n,K-1) \end{bmatrix},\ \mathbf{A}(\theta)=\begin{bmatrix} a_1(\theta_0) & a_1(\theta_1) & \cdots & a_1(\theta_{L-1}) \\ a_2(\theta_0) & a_2(\theta_1) & \cdots & a_2(\theta_{L-1}) \\ \vdots & \vdots & \ddots & \vdots \\ a_N(\theta_0) & a_N(\theta_1) & \cdots & a_N(\theta_{L-1}) \end{bmatrix},$$

$$\mathbf{X}(n)=\begin{bmatrix} x_1(n,0) & x_1(n,1) & \cdots & x_1(n,K-1) \\ x_2(n,0) & x_2(n,1) & \cdots & x_2(n,K-1) \\ \vdots & \vdots & \ddots & \vdots \\ x_N(n,0) & x_N(n,1) & \cdots & x_N(n,K-1) \end{bmatrix},\ \mathbf{N}(n)=\begin{bmatrix} n_1(n,0) & n_1(n,1) & \cdots & n_1(n,K-1) \\ n_2(n,0) & n_2(n,1) & \cdots & n_2(n,K-1) \\ \vdots & \vdots & \ddots & \vdots \\ n_N(n,0) & n_N(n,1) & \cdots & n_N(n,K-1) \end{bmatrix},$$

and θ_l is the direction of arrival of the l^{th} multipath, **A** is the array response matrix, and **N** is the additive white Gaussian noise matrix. In the pre-FFT beamforming, the desired signal vector after passing through the adaptive beamformer with the weight vector **W** is given by

$$\mathbf{s}(n)=\mathbf{W}^H(n)\mathbf{V}(n),$$

where *H* denotes Hermitian transpose. After that the received signal vector is converted into the frequency domain and the signal after FFT is given by

$$\mathbf{y}(n)=\mathbf{F}(n)\mathbf{s}(n)=\mathbf{W}^H(n)\mathbf{V}(n)\mathbf{F}(n)=\mathbf{W}^H(n)\mathbf{U}_p(n),$$

where **F** represents the FFT operation matrix. In [41], the performance and the complexity of the pre-FFT and post-FFT schemes are investigated. The results show that pre-FFT techniques can offer a reliable performance in case there are no strong multipath components in the channel and no strong interference signals. If there are strong multipath components and interferences, post-FFT beamforming is required. Consequently, it is important to verify this observation by a target channel model in use. In general, time domain processing has a low complexity because only one FFT is required [41]. In the frequency domain, spatial signal processing of individual subcarriers is believed to provide the optimum performance but with a much higher complexity. Next, the characteristics of these domains are considered more carefully.

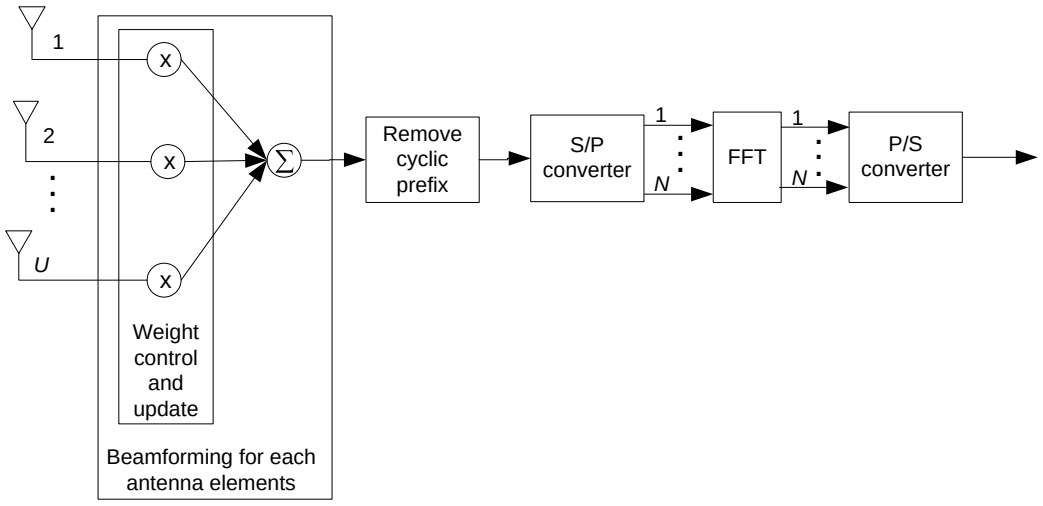

Figure 3.5. OFDM receiver model with adaptive pre-FFT beamformer.

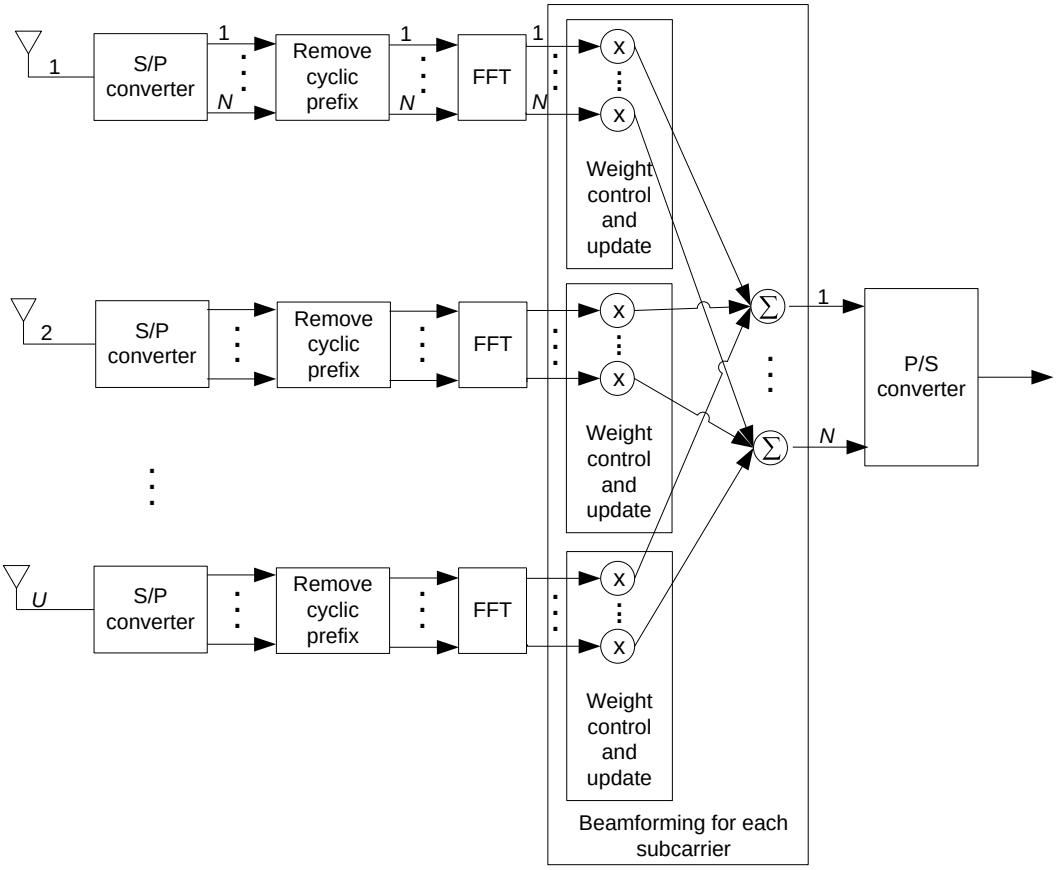

Figure 3.6: OFDM receiver model with adaptive post-FFT beamformer.

3.2.1 Time domain

In [18][19], an algorithm for adaptive pre-FFT beamforming is derived by calculating the pilot error signals in the frequency domain. These error signals are transformed into time domain and the filter coefficients of the adaptive beamformer aiming at minimizing the MSE are updated. Simulation results show that as the number of array elements increase, the BER increases. Furthermore, the convergence becomes faster as the step size increases and the number of pilot symbols increases, but at the cost of loss in bandwidth efficiency. In [37], transmit post-IDFT beamforming and receiver combining are based on the correlation information. Another transmit beamforming scheme is presented in [27]. This transmission structure combines adaptive modulation, space-time block coding, and transmit eigen-beamforming for MIMO-OFDM systems.

A novel pre-FFT OFDM antenna array is proposed for suppressing delayed signals beyond the guard interval [5]. The optimum weight set for the beamformers is based on the maximum SINR and the MMSE criteria. Additionally, a new MMSE-based commutative optimization scheme is proposed that is more robust to the estimation error of the channel state information than the maximum SNIR-based scheme. In [20], pre-FFT beamforming is used with bit and power loading algorithms. Two adaptive LMS beamforming methods were used including the frequency domain and time domain pilot vectors. In [21], pre-FFT technique is used with frequency-to-time pilot transform, and LMS and sample matrix inversion (SMI) algorithms are used for the adaptation. In [23], the same adaptive

beamforming scheme is characterized only by the SMI algorithm. Every OFDM block contains both data and pilot symbols. The frequency domain pilot symbols are transformed into the corresponding time-domain components. Thus, the antenna weight vector of the SMI algorithm can be updated at every OFDM sample instant. This feature can significantly accelerate the convergence of antenna weights. The proposed adaptive beamforming scheme is possible to be used for different sub-bands in post-FFT scenarios to achieve better trade-offs between the complexity and performance. An RLS beamformer was derived for OFDM system with a good convergence performance in [42]. If using such RLS estimator, the frequency domain pilot signal must be transformed into time domain vector first, which needs FFT operations twice to that of [43].

In [43], an adaptive RLS receiver based on pilot symbols in frequency domain is presented. The frequency domain error vector is transformed into time domain because the pilot symbol vector $\tilde{\mathbf{y}}_p(n, i\times\Delta p)$ and the corresponding received pilot signal vector $\mathbf{y}(n, i\times\Delta p)$ are readily available in the frequency domain. The adaptive algorithm for a beamformer is derived by using the following MSE criterion where the squared error between the pilot symbol $\tilde{y}_p(n, i\times\Delta p)$ and received pilot signal $y(n, i\times\Delta p)$ is minimized as

$$E\{\xi_p^2(n)\} = \sum_{i=0}^{N_p} E\left[\left|\tilde{y}_p(n, i\times\Delta p) - y(n, i\times\Delta p)\right|^2\right],$$

where Δp denotes the frequency spacing between pilot symbols and N_p denotes the number of pilot symbols inserted in an OFDM block. It is assumed that the first pilot symbol is positioned at the first subcarrier. Simulation results show that the proposed beamformer has a good convergence performance while reducing computational complexity. Furthermore, it can result in a good BER performance by tracking the channel with a pilot signal.

3.2.2 Frequency domain

In [36], adaptive antenna algorithms based on the SMI algorithm are explored. In OFDM systems, the time-frequency slot contains pilot symbols that permit the SMI calculation to be carried out for interference suppression and equalization of the desired signal. Several strategies are considered for using SMI with different levels of tracking capability over an OFDM time-frequency slot. A new modification to the SMI algorithm was proposed which incorporates the concept of pilot-interpolation into the computation of the sample covariance matrix. This new algorithm is shown to provide a significant improvement to the performance compared with other variations of SMI under consideration.

An adaptive beamforming algorithm based on constant modulus (CM) array, which is a blind beamforming antenna system, is proposed in [34]. It can also appear simultaneously from different directions, thus, it is important that the beamformer weights are updated for each OFDM symbol. The CM array beamforming can adaptively null the co-channel interference by attempting to reconstruct a CM signal. In [9], a new transmit beamforming scheme with limited feedback and beamformer interpolation was proposed. In this scheme, the receiver sends back only a fraction of information about the beamforming vectors along with additional parameters for phase rotation used in the interpolation. A new spherical interpolator is used to calculate the beamforming vectors for all the subcarriers at the transmitter. It was shown that the proposed interpolator can be optimized by

adjusting the parameters for a phase rotation depending on different error rate criteria. A novel blind post-FFT beamforming scheme with a single weight vector applied to all subcarriers in OFDM system is proposed in [8]. The approach assumes that sample synchronization and frequency offset estimation are initially achieved in the scenario with interference. Multiple strong co-channel interferences are present across all subcarriers. Two beamforming techniques are introduced which can effectively cancel co-channel interference even though the power of the interference is strong.

3.3 Performance analysis

In this section, our aim is to evaluate the performance of selected potential beamforming methods in specific UWB channels with an emphasis on mitigating multiuser interferences in multiband MIMO-OFDM systems. The appropriate scenario for mitigating multiuser interferences by using beamforming approaches is illustrated in Figure 3.7. In particular, we consider a virtual MIMO case where other transmitter antennas illustrate interference signals.

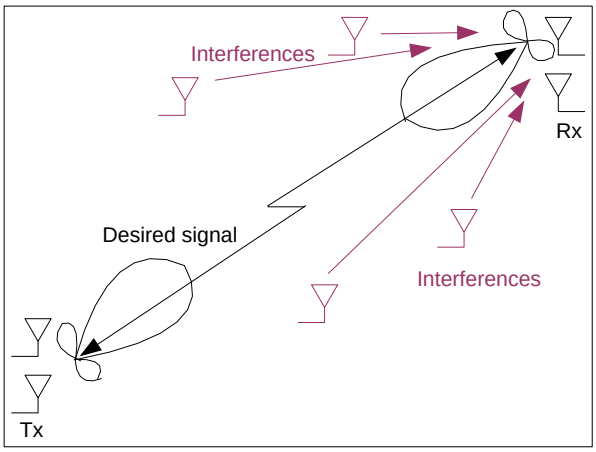

Figure 3.7. Scenario for mitigating multiuser interferences by using beamforming.

3.3.1 Assumptions and used methods

In our interference cases, the interference is of the same kind as the desired signal [14][39]. In the receiver, the received signal can be represented as

$$y_{k,r}(n) = x_k H_k(n) e^{\frac{j2\pi nk}{N}} a_k(\theta_l) + H_{k,r}(n) x_r(r) a_r(\theta_{l_r}) + n_k ,$$

where k is the index of the desired user, r is the index of the interference user, l is index of the multipath component, and n_k is the AWGN noise component. The focus of this study is to analyse two beamforming algorithms, a low complexity pre-FFT and a more efficient post-FFT. Figure 3.8 illustrates the receiver block diagram in the post-FFT case. These algorithms try to separate different simultaneously received signals and successfully detect the desired signal in the OFDM system. The beamforming weights are determined by using an efficient RLS algorithm [43][13] that satisfies the MMSE criterion. The weight vector is updated in the following way:

1) Initialize the update algorithm by setting

$\mathbf{w}(0) = \mathbf{0}$, $\mathbf{R}(0) = \delta^{1}\mathbf{I}$, where δ is a small constant for a high SNR and a large constant for a low SNR.

2) Update the weight vector for $n = n+1$

$$\mathbf{k}(n) = \frac{\mathbf{R}(n-1)\mathbf{u}(n)}{\lambda + \mathbf{u}^H(n)\mathbf{R}(n-1)\mathbf{u}(n)}$$

$$e(n) = d(n) - \mathbf{w}^H(n)\mathbf{u}(n),$$

where $d(n)$ is a reference signal,

$\mathbf{w}(n) = \mathbf{w}(n-1) + \mathbf{k}(n)\mathrm{conj}(e(n))$, and

$$\mathbf{R}(n) = \lambda^{-1}\mathbf{R}(n-1) - \lambda^{-1}\mathbf{k}(n)\mathbf{u}^H(n)\mathbf{R}(n-1),$$

where λ = 0.9990 is a constant forgetting factor.

3) Iterate step 2) until the weight vector converges.

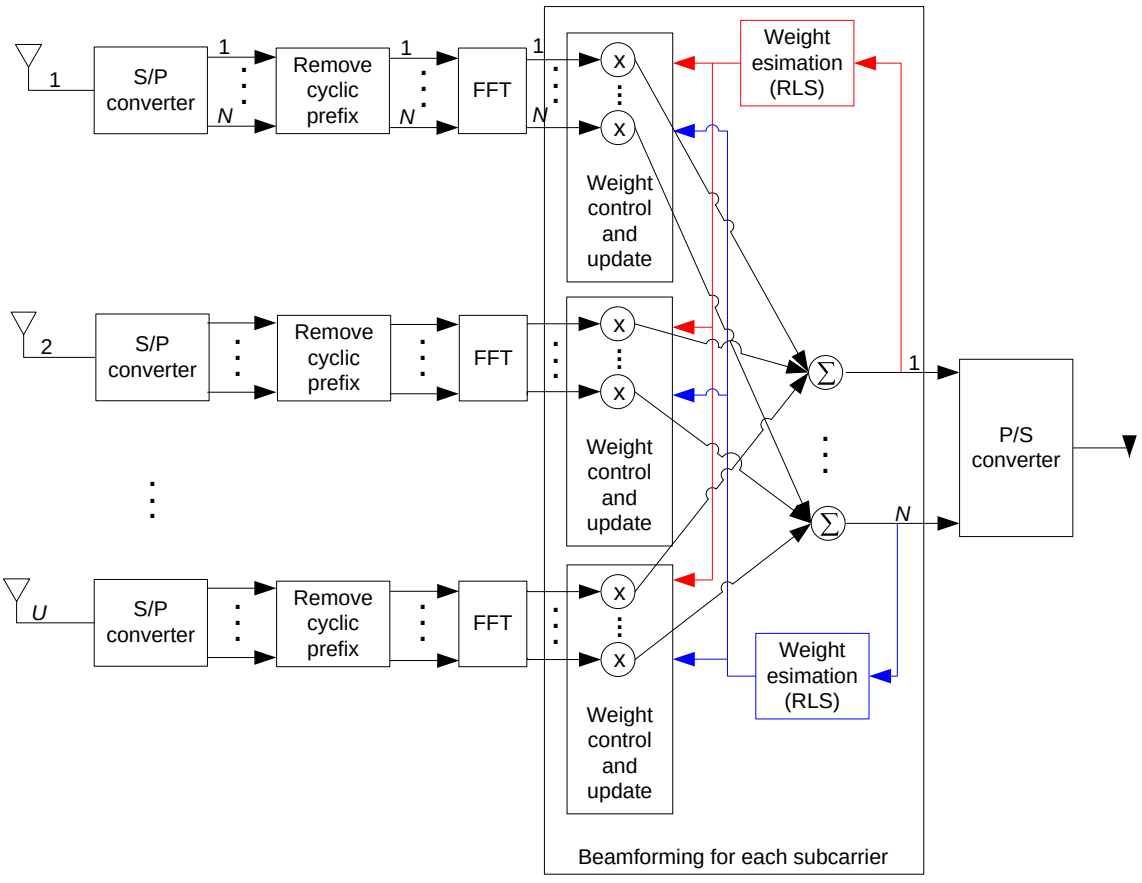

Figure 3.8. Receiver block diagram in post-FFT case.

The simulated system consisted of a transmitter, channel and receiver. Two kinds of channels are considered, namely an AWGN channel and an UWB CM1 channel with lognormal fading. The data

sequence is modulated using either BPSK or QPSK modulation. The other main parameters for the simulation model are given in Table 3.1.

A sequence of information bits was generated in the transmitter using a random data generator, which generates data bits for the whole frame and inserts tailing zeros after each symbol. The generated data sequence was divided into parallel subcarriers. After that each bit in an OFDM symbol is mapped to a unique position in the tones according to the BPSK or QPSK constellation mapping scheme with the channel code rate of one. After constellation mapping, the pilot signal is inserted into the signal. It is inserted into every fifth sample of the data signal (22 pilots/OFDM symbols). Pilot signals are used to calculate the beamforming weights by employing an adaptive RLS algorithm. The signal is transformed into the time-domain using IFFT. Then the guard interval is added to the signal. In the channel, the transmitted signal is corrupted with multiplicative lognormal fading, AWGN, and interference from other users where a selected number of strongest multipath components is chosen and other components are omitted.

In the simulations, the AOAs for the three dominating multipath components are selected as

- desired signal: 10º, 15º, and 5º,
- 1st interference signal: -80º, -85º, and -90º,
- 2nd interference signal: 130º, 134º, and 125º,
- 4th interference signal: -130º, -134º, and -125º,
- 5th interference signal: 150º, 154º, and 145º.

Table 3.1. Parameters of the simulated model**.**

Parameter	**Value**
FFT length	128
Number of symbols	18
Guard interval	37
Number of transmit antennas per user	1
Number of receive antennas per user	4
Antenna element spacing	0.5 **/**
Number of interfering users	0 – 5
Number of dominating multipath components	3-10
Spatial location of the desired signal	0º

In the case when ten dominating multipaths are selected, the AOAs are selected as

- desired signal: 10º, 15º, 5º, 0º, 6º, 12º, 7º, 3º, 14º and 1º,
- 1st interference signal: -80º, -85º, -90º, -75º, -70º, -82º, -88º, -72º, -83º, and -87º,
- 2nd interference signal: 130º, 134º, 125º, 128º, 120º; 127º, 132º, 122º, 124º, and 129º,
- 3rd interference signal: 80º, 84º, 72º, 76º, 90º, 82º, 88º, 73º, 83º, and 87º
- 4th interference signal: -130º, -134º, -125º, -128º, 120º, -127º, -132º, -122º, -124º, and -129º.

At the receiver side, the guard interval between the OFDM symbols is first processed to form the information data sequence. After that, the signal is filtered by using the described RLS algorithm. The beamforming weights are defined based on the pilots and the received signals of the antenna elements are multiplied by the weights.

3.3.2 Numerical results

BER simulation results are first evaluated in an AWGN channel to act as a lower bound reference. Figure 3.9 shows three interference cases for the BPSK modulation scheme and Figure 3.10 shows the corresponding results for the QPSK modulation scheme. Theoretical curves illustrate BER for an AWGN channel in a single antenna case. The interference mitigation works quite well when the number of interference sources is less than the number of receive antennas. We can see that if the number of interference sources is higher than the number of antenna elements, the beamformer cannot compensate interferences. We can also notice that when the number of interference sources is the same as the number of the antenna elements, the performance is already clearly degraded.

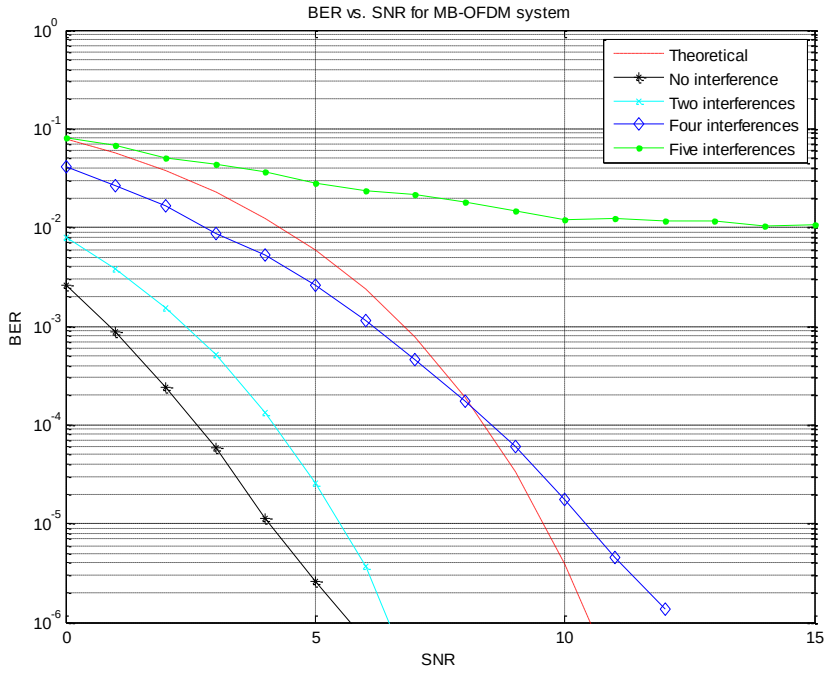

Figure 3.9. BER for RLS-beamformed BPSK in different interference scenarios with AWGN.

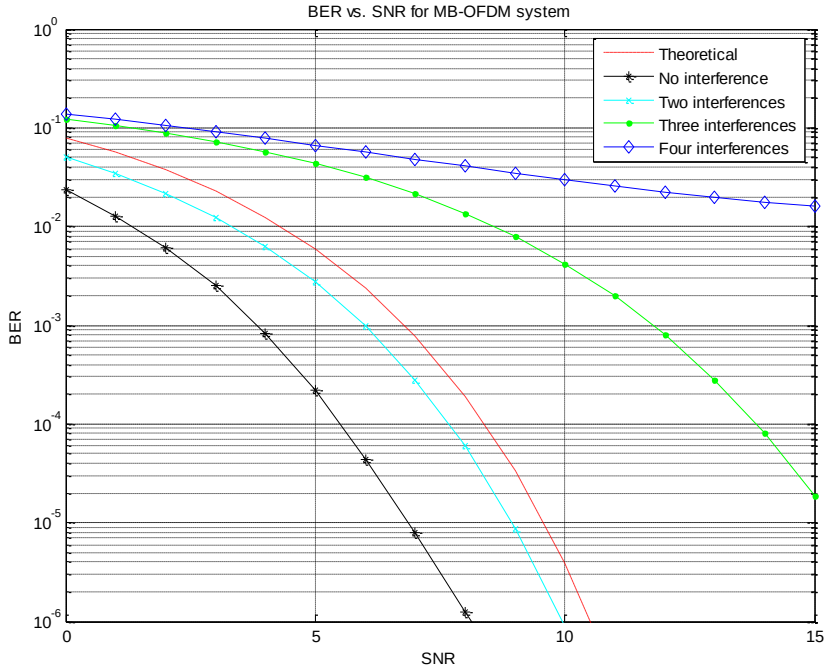

Figure 3.10. BER for RLS-beamformed QPSK in different interference scenarios with AWGN.

The next simulation results illustrate the cases for a lognormal UWB multipath fading channel where the three strongest multipath components are selected to be nulled. Figure 3.11 shows six interference cases for the BPSK modulated pre-FFT OFDM scheme where the number of the antennas and interferences are changed to represent different scenarios. Results show that the interference can be mitigated if the number of received antennas is higher than the number of interferences plus number of multipath components. However, the achieved BER level is only 0.01 when the maximum number of interferences and multipath components are used. It seems that the pre-FFT beamforming cannot mitigate well the wideband interferences in lognormal UWB multipath fading channels. Figure 3.12 illustrates the same situation as in Figure 3.11, except that the QPSK is used. We can see that we need six antenna elements to achieve an acceptable performance in one interference case. Moreover, nine antenna elements are needed to mitigate the effect of the interferences in the case of two interferences.

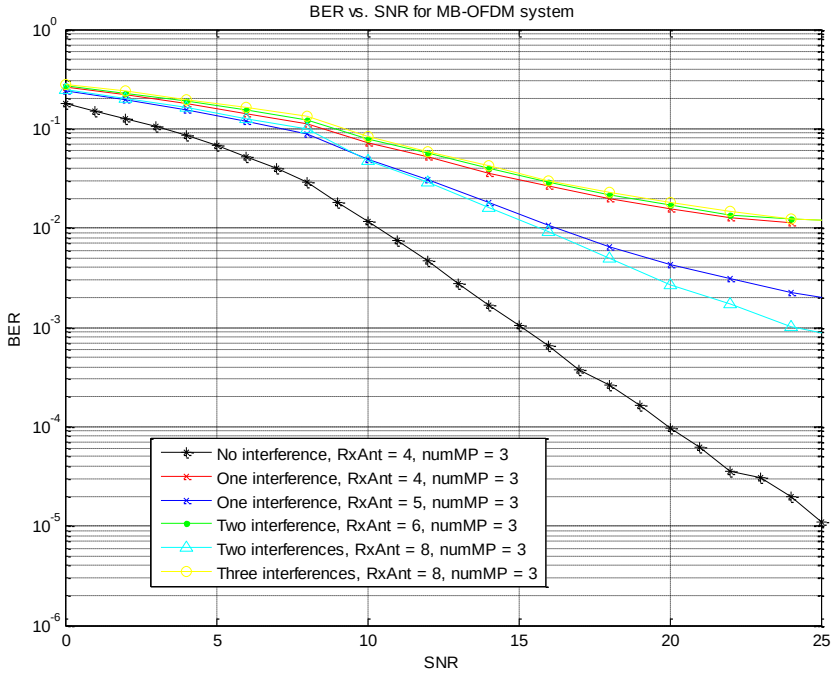

Figure 3.11. BER for pre-FFT-RLS-beamformed BPSK modulation in multipath UWB channel with equal interference power desired signal power.

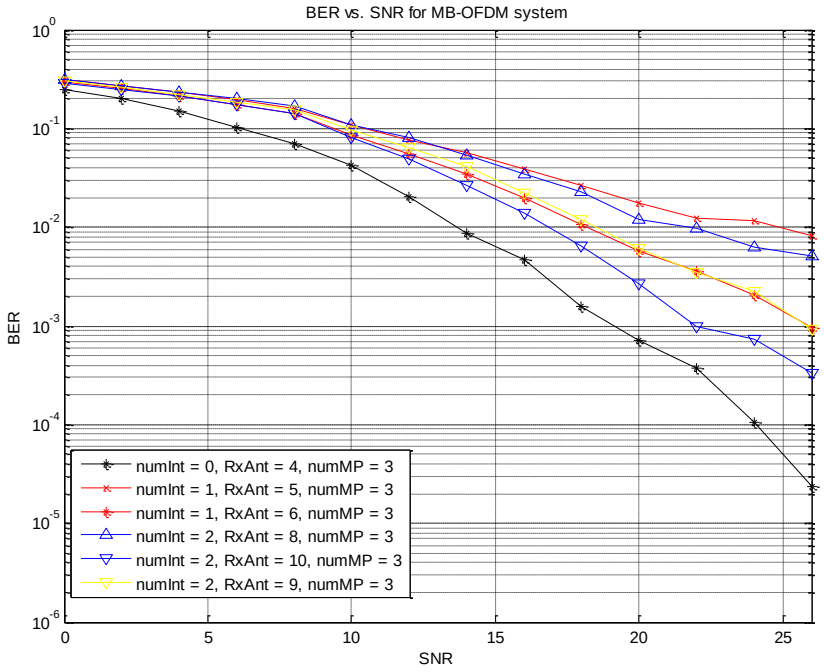

Figure 3.12. BER for pre-FFT-RLS-beamformed QPSK modulation in a multipath UWB channel with equal interference power desired signal power.

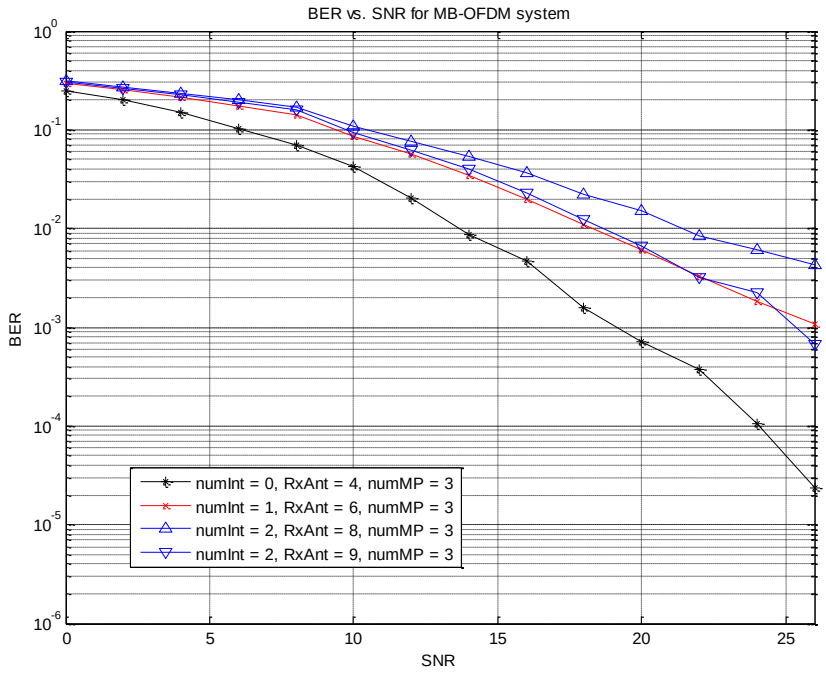

Figure 3.13. BER for pre-FFT-RLS-beamformed QPSK modulation in multipath UWB channel with 50 % interference power of the desired signal power.

Figure 3.14 illustrates interference cases for the BPSK-modulated post-FFT OFDM scheme where the number of the elements and interferences are varied to represent different interference scenarios. We observe that the performance of the post-FFT beamformer is better than that of the pre-FFT beamformer because each subcarrier has its own beamforming weights in the post-FFT scheme. We further observe that the BER of 10^{-3} is achieved when the number of interferences is less than three. Then, the number of the antenna elements is the same as the number of the interferences plus multipath components. When the number of interferences is four, the number of antenna elements in the receiver has to be nine to achieve a good performance. Figure 3.15 illustrates interference cases for the QPSK modulated post-FFT OFDM scheme. The number of the interferers is varied from zero to five. We observe that the post-FFT beamformer can mitigate the effects of the interferences if the number of the interferences is less than five.

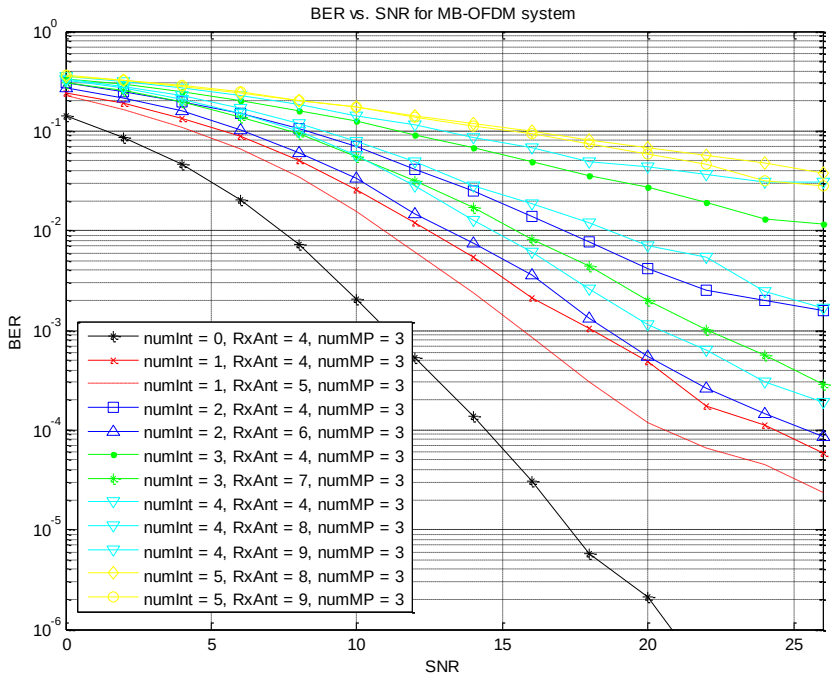

Figure 3.14. BER for post-FFT-RLS-beamformed BPSK modulation in a multipath UWB channel with equal interference power of the desired signal power.

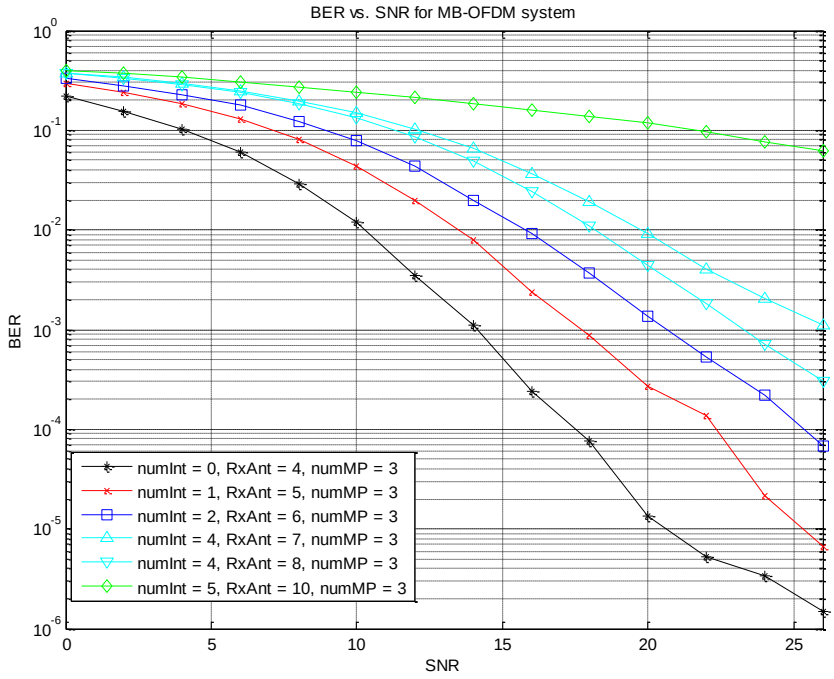

Figure 3.15. BER for post-FFT-RLS-beamformed QPSK modulation in a multipath UWB channel with equal interference power of the desired signal power.

In Figure 3.16, the simulation cases are the same as previously but the power of the interference is decreased. In these simulations, the power of the interference is 50 % of the power of the desired signal which represents the case in which the interference sources are farther away from the receiver in comparison with the desired signal source. We note that the performance is now better than in Figure 3.15. In Figure 3.17, the power of the interference is now increased. It is 200 % of the power of the desired signal representing the case in which the interference sources are closer to the receiver in comparison with the desired signal source. We note that the effects of the interference are much stronger compared to the cases in which the power of the interference is 50% or 100% of the desired signal.

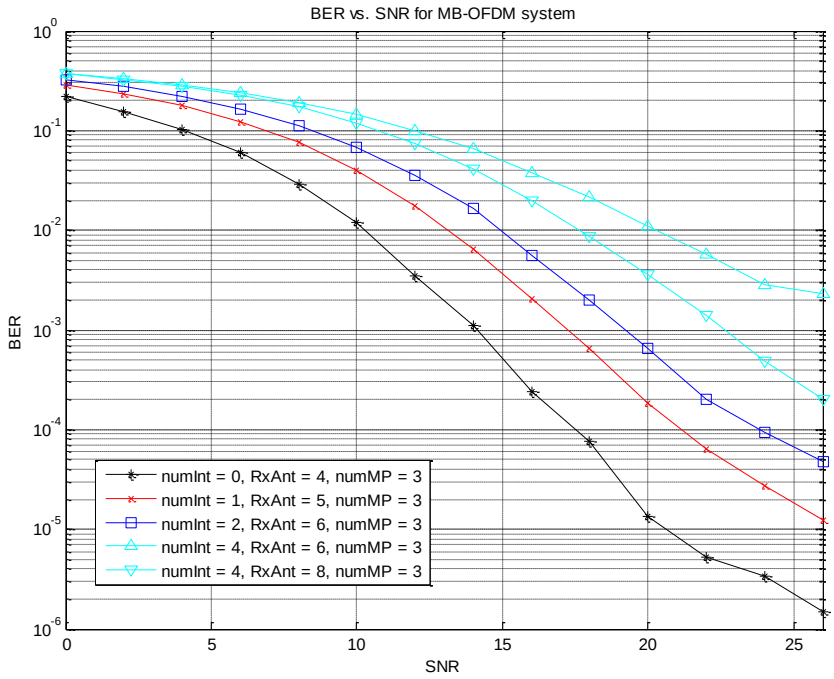

Figure 3.16. BER for post-FFT-RLS-beamformed QPSK modulation in multipath UWB channel with 50 % interference power of the desired signal power.

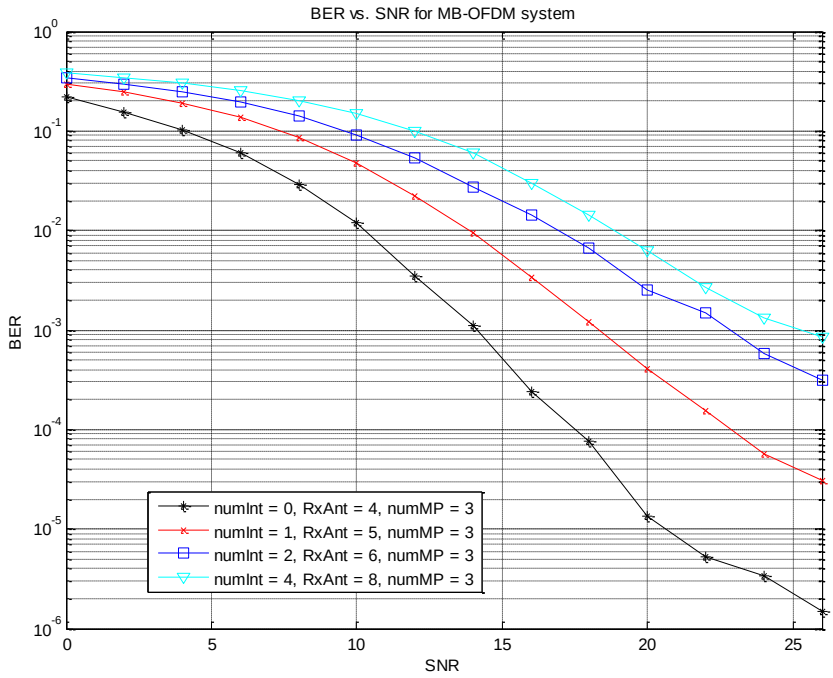

Figure 3.17. BER for post-FFT-RLS-beamformed QPSK modulation in multipath UWB channel with 200 % interference power of the desired signal power.

Figure 3.18, Figure 3.19, and Figure 3.20 illustrate the same case as previously except that the number of considered strongest multipath components is increased to ten. We can note that when the power of the interference is the same as the power of the desired signal, we need five antenna elements to achieve the BER performance of 10^{-3} as can be seen in Figure 3.18. Additionally, when two interference signals disturb the transmission, six antenna elements are needed, and ten antenna elements are needed in the case with four interference signals. In Figure 3.19, we observe that the performance is significantly better than in Figure 3.18, because in this case the power of the interference signals is half of the desired signal. In Figure 3.20, we observe that the effects of the interferences become most severe since the power of the interference signal is the highest.

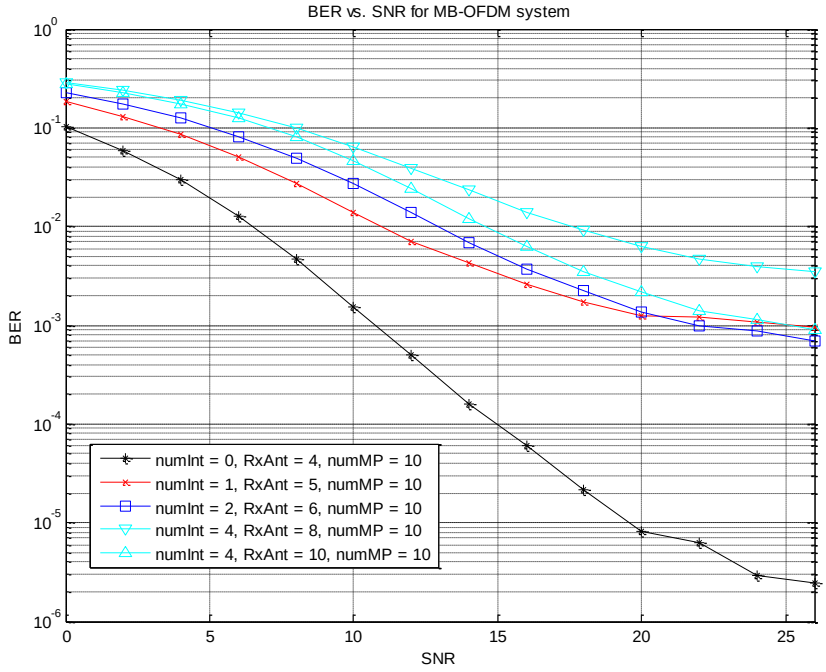

Figure 3.18. BER for post-FFT-RLS-beamformed QPSK modulation in multipath UWB channel with equal interference power and desired signal power.

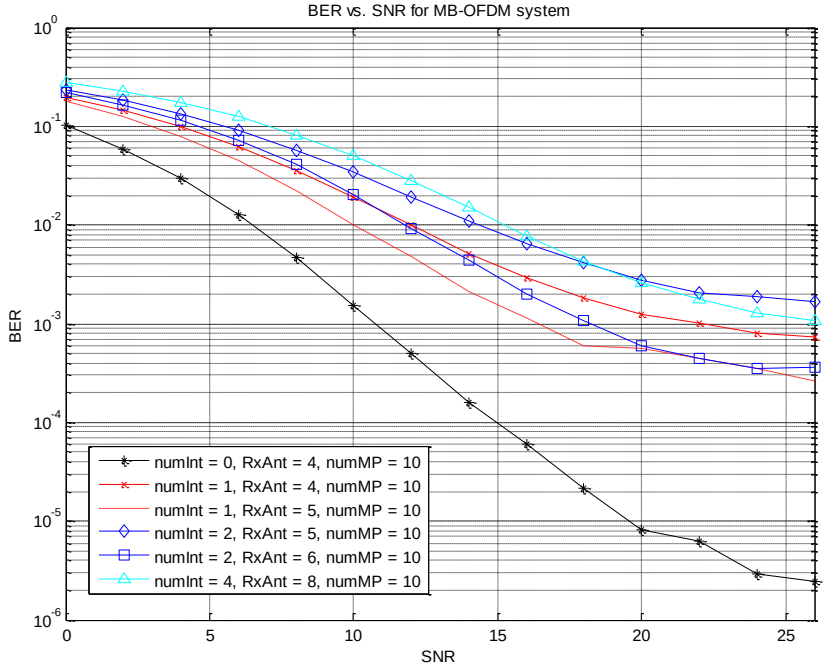

Figure 3.19. BER for post-FFT-RLS-beamformed QPSK modulation in multipath UWB channel with 50 % interference power of the desired signal power.

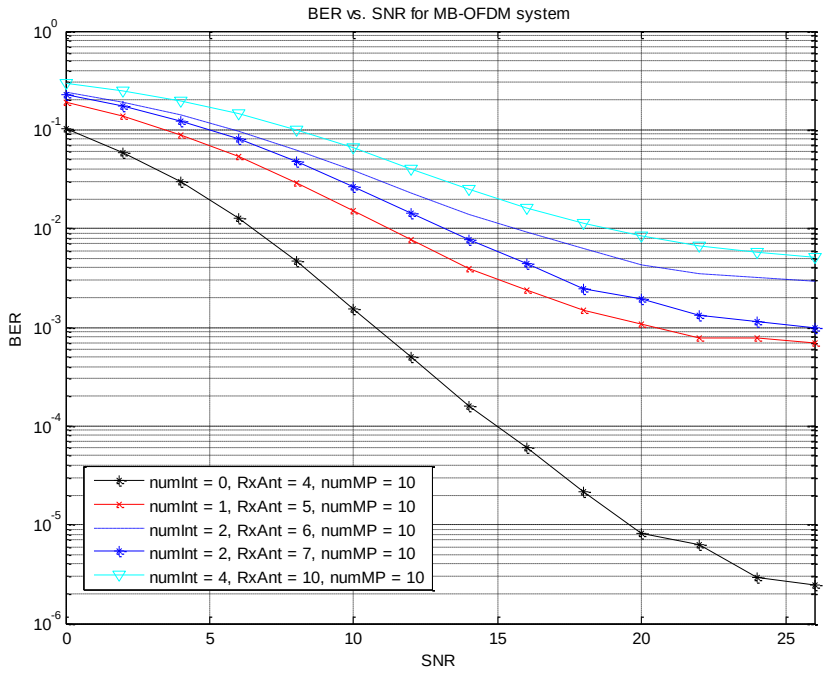

Figure 3.20. BER for post-FFT-RLS-beamformed QPSK modulation in multipath UWB channel with 200 % interference power of the desired signal power.

A major conclusion from our study is that the investigated pre-FFT beamformer seems to be more vulnerable to the interference signals than the post-FFT beamformer in UWB multipath fading channels. One reason for this is that the post-FFT beamformer transforms the wideband signal into the narrowband signal, because beamforming is made after FFT operation. Thus, each subcarrier has its own coefficient of beamformer. In the pre-FFT case, each antenna has only one coefficient per beamformer. However, the trade-off implies the post-FFT method is more complicated than the pre-FFT approach.

4 Time-reversal techniques

In the following, we introduce the concept of UWB Time Reversal (TR) techniques and argue on their importance for our MIMO-UWB system. In particular, we present the conceptual description of the UWB beamforming with TR pre-filtering technique considering the methodology and major challenges.

4.1 Time Reversal in UWB

The time reversal combined with wideband signals is proposed in rich multipath propagation scenarios to achieve temporally and spatially focusing gain. The time focusing ability reduces the Inter-Symbol Interference (ISI) and maximizes the output SNR within small time duration [46]. In addition, the spatial focusing on intended target will minimize the multi user interference (MUI).

The TR filter is the temporal reverse of the channel impulse response (CIR). Assume a channel $h(t) = \sum_{l=0}^{l=L-1} h_l \delta(t - l\Delta T)$ of length L, where ΔT is the sampling interval. The cascade of the TR filter and the propagation channel can be seen as an equivalent channel $\hat{h}(t)$ and is the autocorrelation of the CIR.

$$\hat{h}(t) = h(t) \otimes h(-t)$$

Since the receiver samples the signal at time instant $t = (L-1)\Delta T$, the equivalent channel can be considered as a flat fading channel. This viewpoint will be used to deal with UWB/WB beamforming problem.

4.2 Beamforming and TR pre-filtering

The proposed approach consists of two-layer processing: an *inter-layer* and an *outer-layer*. In the inter-layer, the TR Pre-Filtering technique is applied to the TX UWB for the channels from the TX UWB to both the RX UWB and other wireless victim devices. In the outer-layer the Zero-Forcing (ZF) beamforming technique [49] is applied to the multiple antenna UWB Base Station (BS) in order to null the interference to the victim users. As mentioned above, the TR spatially focusing ability can help reducing the (MUI). However, for highly correlated channels the spatially focusing gain will incur severe degradation. The pre-filtering ZF beamforming algorithm is thus proposed in order to ensure the interference mitigation to the victim users and to enhance the system reliability. The combining of the ZF beamforming technique with the TR Pre-Filtering makes use of the following advantages. First the TR filter achieve maximum output SNR as it is designed as a matched filter at transmitter side and reduce the ISI due to the temporally focusing gain. Second, the cascade of the TR filter and the propagation channel can be modelled at the instant time $t = (L-1)\Delta T$ as a flat fading channel with a single tap. This viewpoint allows applying the current beamforming technique to this single tap, which yields to a significant reduction of the system complexity. Third, the ZF beamforming algorithm reduces the MUI.

4.3 Mathematical Framework

We consider a MU-MIMO UWB system (Figure 4.1) in which a single transmitter is equipped with M antennas transmitting to K decentralized users. Each RX user is equipped with only one antenna. For the channel between the UWB TX equipped by M antennas and the users' receivers provided by $N=1$ receiving antennas we assume multipath propagation. The maximum length of the discretized $NU\acute{}\ M$ multipath channel realizations is assumed to be L taps. At a time instant *k*, the propagation channel could be described as [48],[49]

$$\mathbf{H}[k]=\begin{bmatrix} h_{11}[k] & h_{12}[k] & \dots & h_{1M}[k] \\ h_{21}[k] & h_{22}[k] & \dots & \dots \\ \dots & \dots & \dots & \dots \\ h_{K1}[k] & h_{K2}[k] & \dots & h_{KM}[k] \end{bmatrix}$$

Suppose a TR filter for the system is applied at the transmitter with the filtering matrix given by

$$\overline{\mathbf{H}}[k]=\begin{bmatrix} \overline{h}_{11}[k] & \overline{h}_{21}[k] & \dots & \overline{h}_{U1}[k] \\ \overline{h}_{12}[k] & \overline{h}_{22}[k] & \dots & \dots \\ \dots & \dots & \dots & \dots \\ \overline{h}_{M1}[k] & \overline{h}_{2U}[k] & \dots & \overline{h}_{MU}[k] \end{bmatrix}$$

the equivalent flat fading channel is defined as:

$$\hat{\mathbf{H}}[k]=\begin{bmatrix} \hat{h}_{11}[k] & \hat{h}_{21}[k] & \dots & \hat{h}_{U1}[k] \\ \hat{h}_{12}[k] & \hat{h}_{22}[k] & \dots & \dots \\ \dots & \dots & \dots & \dots \\ \hat{h}_{1U_D}[k] & \hat{h}_{2U_D}[k] & \dots & \hat{h}_{UU_D}[k] \end{bmatrix}.$$

The length of the equivalent channel is $L_e = 2L - 1$.

Consider a block of received signal at time instants $k, k+1, \dots, k+K-1$, respectively, which is presented as

$$\mathbf{y} = \mathbf{H}_{eq}\mathbf{x} + \mathbf{n}$$

where

$$\mathbf{x} = \frac{1}{\sqrt{M}}[\mathbf{x}^T(k-L_e+1), \mathbf{x}^T(k-L_e+2), \dots, \mathbf{x}^T(k), \dots, \mathbf{x}^T(k+K-1)]^T$$

$$\mathbf{y} = [\mathbf{y}^T(k), \mathbf{y}^T(k+1) \dots, \mathbf{y}^T(k+K-1)]^T$$

$$\mathbf{n} = [\mathbf{n}^T(k), \mathbf{n}^T(k+1) \dots, \mathbf{n}^T(k+K-1)]^T$$

Due to the temporal-focusing property of the equivalent channel, a shortened equivalent channel matrix $\mathbf{H}_{eq,S}$ is defined. Let the tap index for the peak tap be k_p, $\hat{\mathbf{H}}[k_p]$ is selected as the CIR matrix of the shortened equivalent channel.

When $M \geq NK$, the ZF beamforming weight matrix can be calculated as [48]

$$\mathbf{W} = \alpha \, \mathbf{H}_{eq,S}{}^{T} (\mathbf{H}_{eq,S} \mathbf{H}_{eq,S}{}^{T})^{-1}$$

where $(.)^{T}$ denotes the conjugate transpose.

Note that the pre-equalizer will be applied to the data stream to the desired users. The coefficient α is introduced for the power constraint of the transmit signal and is computed according to the FCC mask.

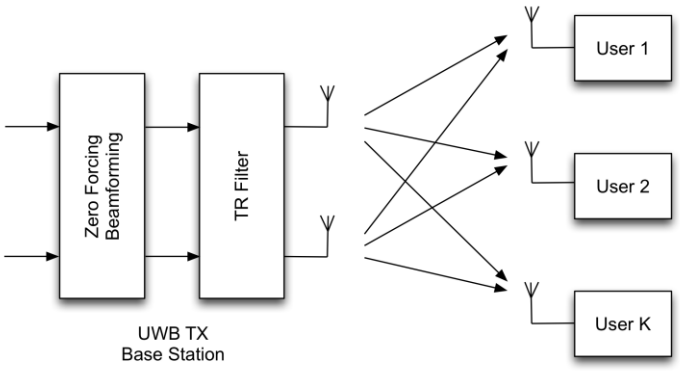

Figure 4.1. Block diagram of the multi-user scenario.

4.4 Numerical Results

The ray tracing setup used to simulate the propagation channel in the MU-scenario is depicted in Figure 4.2. Two UWB base stations BS1 and BS2 are equipped by 4 antennas for each base station, whereas 3 users equipped with only one antenna have been considered.

In the simulation setup, the maximum numbers of reflections, transmissions and diffractions were 3, 1 and 1 respectively, while a power threshold of -150 dB was used for the considered paths. The maximum length of the generated CIRs is limited to $L = 500$ taps.

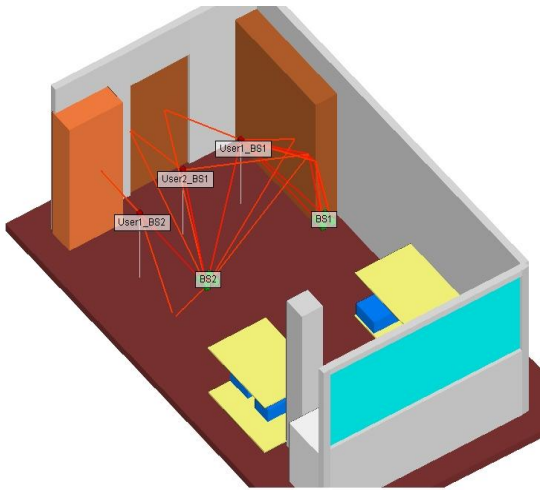

Figure 4.2. Ray Tracing setup: Two UWB base stations BS1 & BS2 (green) each had 3 antennas and 3 users (red) each is equipped with one single antenna and distributed in an indoor office environment.

A multi-user UWB-IR scenario has been considered and two different bit streams are exciting the BS1 while a third different bit stream is exciting BS2. Binary data is modulated by PPM schemes and shaping using a Gaussian pulse

$$p(t) = \left[1 - 4\pi\left(\frac{t - t_m}{\tau}\right)^2\right] e^{-2\pi\left(\frac{t-t_m}{\tau}\right)^2},$$

where $t_m = 0.45$ ns and $t = 0.25$ ns. It is assumed that the signal is perfectly synchronized at the receivers.

Figure 4.3a) shows the equivalent channel $\hat{h}(t)$ resulting from the convolution between the time reversal channel and its corresponding UWB CIR of user USR2-BS1 which could be described mathematically as the first element of the diagonal of the equivalent channel matrix $\hat{\mathbf{H}}$ computed at the BS1, while Figure 4.3b), c) cross-correlation between the time reversal channel and the other non-relevant CIRs. This could be also mathematically described as the other non-diagonal elements comprising the interference.

A fair comparison of the BER vs. SNR curve at a certain user USR1 in the UWB multi-users system with/without applying pre-filtering ZF beamforming at the antennas of BS1 for mitigating the interference between the different users is illustrated in Figure 4.4. In the meanwhile it is concluded that increasing the number of transmitting antennas from 3 to 4 can provide a diversity gain.

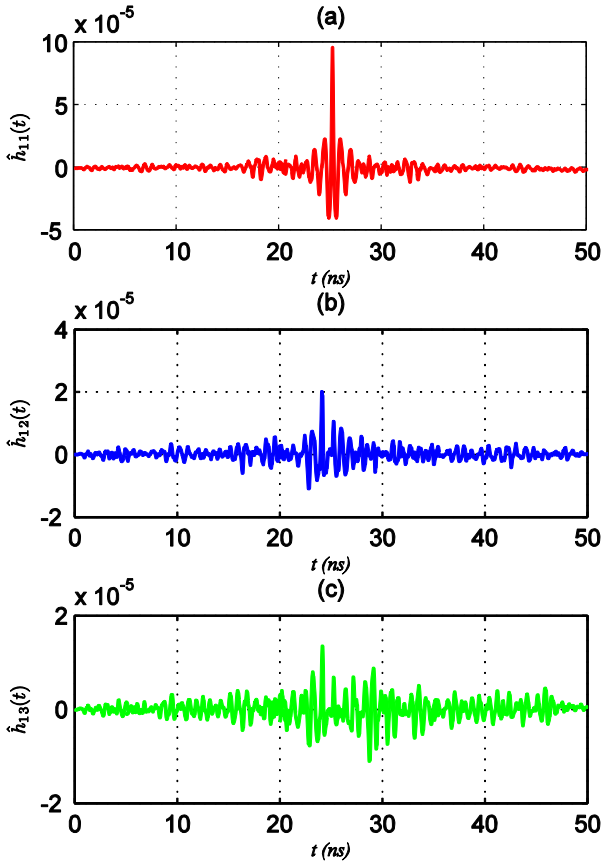

Figure 4.3. Equivalent channel $\hat{h}(t)$ resulted from (a) the convolution between the time reversal channel and its corresponding UWB CIR of user USR2-BS1 and (b, c) cross-correlation between the time reversal channel and the other two non-relevant CIRs of the other two users USR1-BS1 and USR1-BS2.

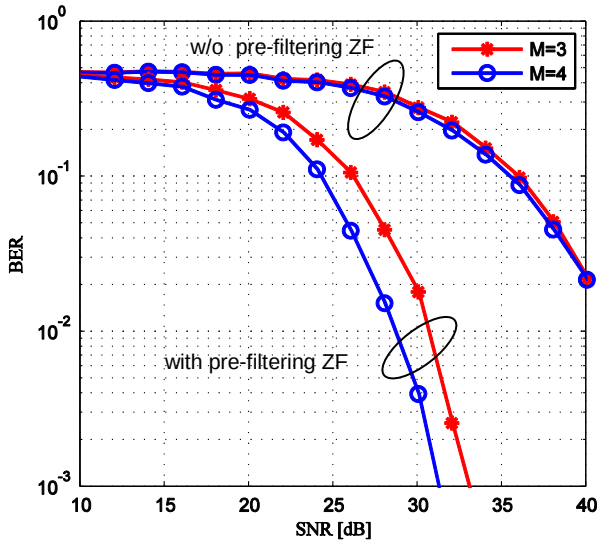

Figure 4.4. A comparison of the BER vs. SNR curve at a certain user USR1 in the UWB multi-users system with/without applying pre-filtering ZF beamforming at the antennas of BS1 for mitigating the interference between the different users.

5 Interference mitigation techniques

Due to its "underlay" nature, UWB technology has to ensure the coexistence with other services operating in the same frequency range. This implies UWB being able to detect and possibly avoid such primary users and to adjust its parameters respectively so that no harmful interference is caused at victim receivers.

5.1 Co-existing scenario between and WiMAX

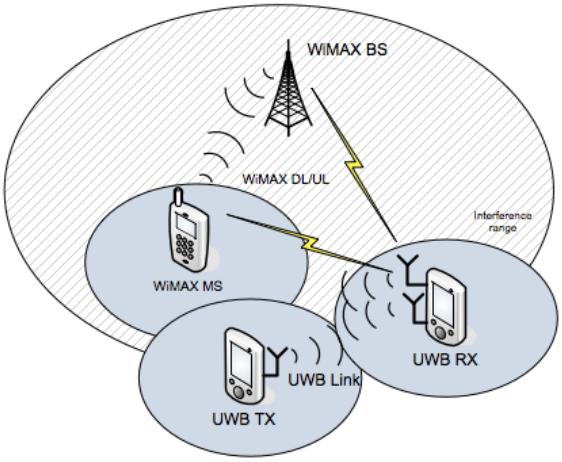

Figure 5.1. Co-existing scenario between UWB and WiMAX.

To demonstrate the DAA capabilities of UWB technology, we consider the following example of an interference scenario: A primary user (WiMAX mobile terminal) operates in close proximity of two communicating UWB devices, see Figure 5.1. During its start-up, the UWB communication system performs a spectrum scan of the environment to possibly detect and mitigate its negative influence and thus allow for peaceful co-existence with licensed narrow-band services in its proximity. ECC TG3 have recently proposed a so-called flexible zone model for DAA, according to which the space around the victim receiver is separated in different zones depending on the received power of a primary user [50],[51]. Depending on the detected interference level, the UWB device applies some mitigation technique, e.g. dropping a sub-band, tone nulling or notch-filtering. Further, the presented DAA procedures can be sophisticated to include coherent spectrum sensing and monitoring phase to better estimate the isolation distance from the victim receiver and reduce the overhead for scanning the whole environment.

Table 5.1. Parameters of the WiMAX interference scenario.

Parameter	**Value**
WiMAX TX UL power	20 dBm
WiMAX Bandwidth	5 MHz
WiMAX min DL sensitivity	-90 dBm
WiMAX Noise Figure (NF)	5 dB

WiMAX carrier frequency	3.5 GHz
SIR at WiMAX RX	- 6 dB
Thermal noise	-114 dBm/MHz
WiMedia signal level	-41.3 dBm/MHz
WiMedia Noise Figure	6.6 dB
Protection level	-60 dBm/MHz -65 dBm/MHz
Channel availability check-time	<= 50 ms

Table 5.1 summarizes the main set-up parameters for the proposed WiMAX interference test scenario. Since the required WiMAX DL sensitivity (detection level) is -90 dBm or -97 dBm/MHz, the interferer lies only 10.4 dB (= -97 - 6.6 + 114) above the WiMedia noise floor. The challenging task of detecting the victim signal in harsh multipath environment and shadowing effects may be alleviated by increasing the integration period of the detection algorithm, using some a-priori knowledge of the interfering system or exploiting the intrinsic receive diversity via multiple antennas.

5.2 Differential algorithm for interference energy detection and mitigation

In this section we propose a differential algorithm for a non-coherent energy detection of narrowband signals incorporated in the MB-OFDM receiver. As specified in the interference scenario (see Table 5.1), the detection of a 5 MHz signal is considered, whereas the energy detector accumulates the FFT bins over a multiple MB-OFDM symbol slots. The output of the detector is differentially compared with a detection threshold, and the bins that result in positive hypothesis tests indicate the presence of WiMAX transmissions.

The UWB receiver can employ the detection function to listen continuously for WiMAX emissions during the start-up phase. A detection phase of 30 up to 70 symbol slots is considered sufficiently long to detect reliably the WiMAX UL/DL signal. In case the UWB device fails to detect the victim device during this initial check, it will continue to monitor the environment on an on-going base, e.g. during the beaconing phase or the transmission-free intervals between two data frames.

The flow chart of the proposed interference detection scheme is shown in Figure 5.2. The algorithm takes as parallel input the averaged FFT bins over all RX antennas during a set number of slots. Depending on the time-frequency hopping pattern, the symbol blocks are accumulated in a normalized power array of length 3*128 tones, corresponding to up to three sub-bands within a band group. Each power bin is decremented by the average of the preceding bins and then compared with a detection threshold. If the power of this differential bin exceeds the threshold, its index is output, while its value is neglected for the calculation of the supplementary moving sum *P_sum* over the bins. In case a bin value lies below the threshold, the moving sum is incremented by its value, after which the value is replaced by the increment of the moving sum, see Figure 5.2.

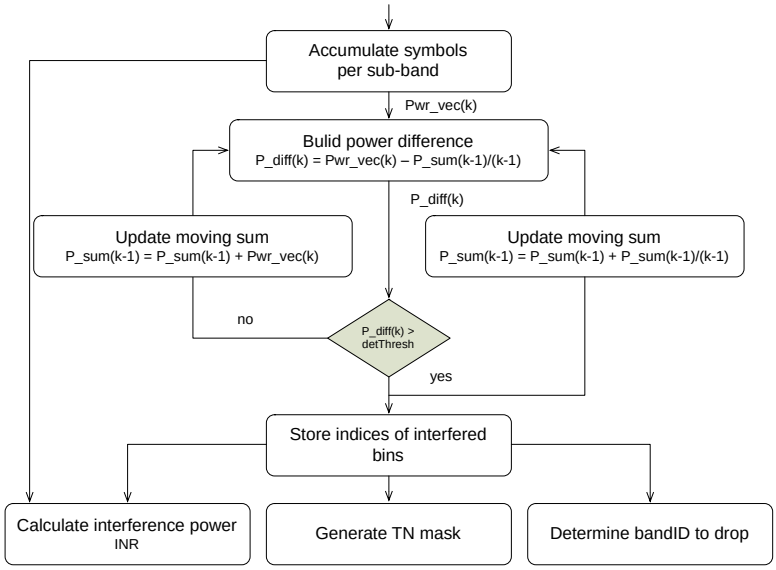

Figure 5.2. Flow diagram of per-bin differential interference detection.

In case of successful detection, the sub-band(s) corresponding to the detected interferer index is determined and output for the application of e.g. band dropping techniques at the TX. Further, a tone-nulling (TN) mask of length 3*128 is generated, containing 1's for each sub-carrier to be transmitted, and 0's for the tones to be zeroed. Variable number of guard tones are zeroed on both sides of the detected bin in order to allow deeper notching of the transmit UWB signal.

Finally, the power level of the detected interferer and Interference-to-Noise ratio are estimated, and a flag for successful detection is output. The power of the interferer may then be used to determine the interference zone and required isolation to the victim device.

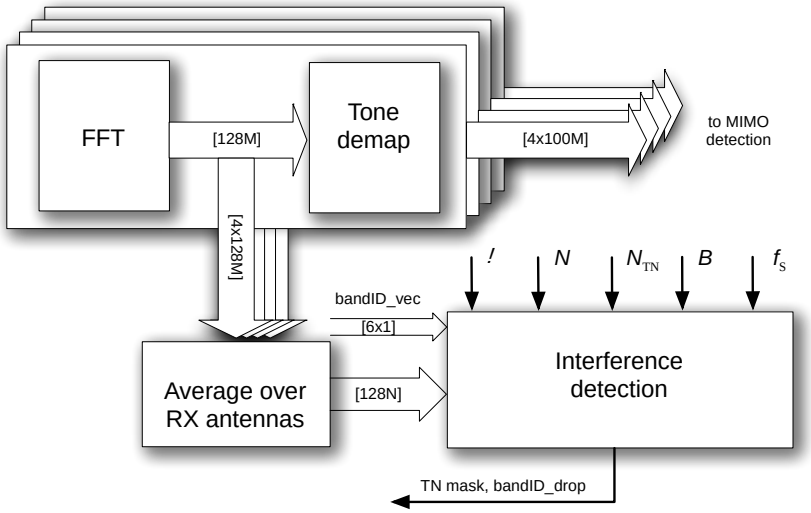

Figure 5.3. Block diagram of interference detection.

In order to verify the performance of the per-bin interference detector, we consider a MIMO MB-OFDM receiver deploying 4 antennas. The inter-connections of the interference detection block with

e.g. the multiple FFT-, Tone mapping and symbol averaging block are shown in Figure 5.3. The output bins of the FFT blocks are first averaged over the 4 RX antennas and then fed in serial to the interference detection block. The size of this input stream is 128N tones/bins, where N stands for the number of slots/symbols the detection is to be carried over. The bandID_vec array specifies the time-frequency hopping pattern of the receiver and contains 6 values for 6 consecutive time slots. The parameters h, N, N_{TN}, B, and f_S define the normalized detection threshold, number of tones per slot, number of TN guard tones, system bandwidth and sampling frequency respectively. The output of the detection block is a 3*128 TN mask, an index of the sub-band to be dropped, average interferer power level and estimate of the Interference-to-Noise ratio.

For testing purposes, we applied simple Band Dropping and Tone Nulling algorithms at the transmitter after performing a spectrum sensing and interferer detection during start-up. Figure 5.4 summarizes the performance results for a MB-OFDM system operating in 480 Mbps DAA-mode in the close proximity of a WiMAX mobile device. Both avoidance techniques still preserve reliable UWB communication while ensuring the desired protection level (isolation) to the victim device. Each additional antenna at the RX provides an intrinsic array gain of up to 3 dB as compared to a single antenna case.

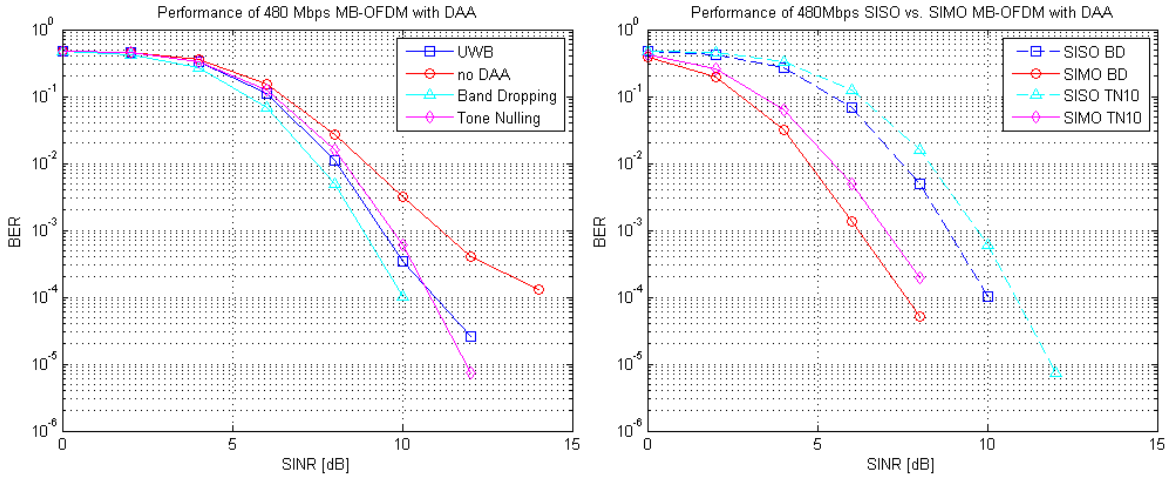

a) b)

Figure 5.4. Performance of a) SISO and b) 1x2 SIMO 480 Mbps MB-OFDM with DAA in the presence of WiMAX interferer.

The probabilities of interference detection (*False Alarm*, *Missed Detection*) vs. a normalized threshold are presented in Figure 5.5. We concluded that suitably low levels of missed detection and false alarm probabilities can be reached by integrating over 30 MB-OFDM symbols, allowing reliable and fast detection of a WiMAX uplink for low levels of the interference-to-noise ratio (INR).

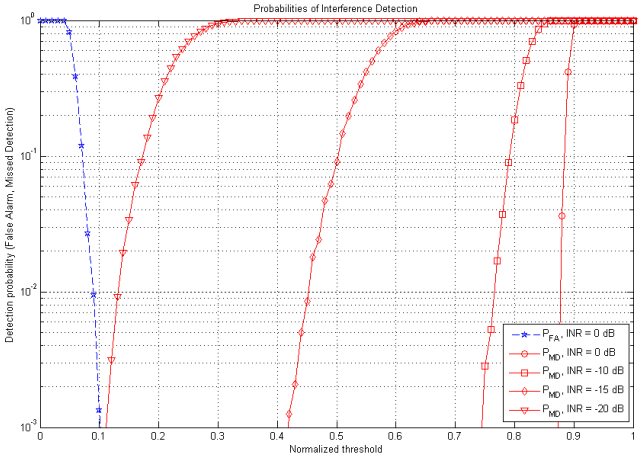

Figure 5.5. Performance of WiMAX interference detection.

6 Conclusions

In this report, we have addressed several approaches to mitigate multiuser interference in short-range UWB communication channels. Multiuser interference is one of the most detrimental effects reducing the efficiency of current short-range communication applications, giving motivation for further research on this topic.

Regarding the beamforming approach, an extensive overview of existing schemes and their trade-off analysis was provided first. We then focused on a specific recursive least squares method, which was found to be an appealing adaptive solution to estimate the beamforming weights for mitigating the multiuser interference in OFDM-based UWB systems. Interesting study cases were identified with an emphasis to compare time- and frequency-domain beamforming approaches at the receiver. Extensive simulation study was then conducted in the selected UWB channels with different interface scenarios, and it is found that the frequency-domain beamforming approach is more effective than the time-domain approach at the cost of increased complexity.

Further, time-reversal technique has been applied in order to reduce the effect of the inter symbol interference significantly without the need for high complexity equalizer at the receiver. TR in impulse radio UWB transmissions is one viable solution to improve the multi-user system capacity and communication range. Combining the ZF beamforming technique with TR pre-filtering achieves maximum output SNR as it is designed as a matched filter at the transmitter side and reduces the ISI due to the temporally focusing gain. The cascade of the TR filter and the propagation channel can be modelled at the sampling time as a flat fading channel with a single tap. This viewpoint allows applying the current beamforming technique to this single tap, which yields to a significant reduction of the system complexity.

Finally, co-existence and interference testing results in the presence of WiMAX demonstrate the functionality of a flexible DAA approach based on spectrum sensing, band dropping or tone nulling to mitigate the harmful interference to victim systems.

References

[1] F. Alam, B. L. P. Cheung,R. Mostafa, W. G. Newhall, and J. H. Reed, "Sub-band Beamforming for OFDM System in Practical Channel Condition," *Proceedings VTC 2004-Fall*, vol. 1, pp. 235 – 239, 2004.

[2] A. Batra, J.Balakrihnan, G. R. Aiello, J. R. Foerster, and A. Dabak, "Design of a Multiband OFDM System for Realistic UWB Channel Environments," *IEEE Transactions on Microwave Theory and Techniques*, vol. 52, no. 9, pp. 2123 – 2138, November 2004.

[3] J. Benesty, J. Chen, and Y. Huang, *Microphone Array Signal Processing*, Springer Berlin Heidenberg, 2008, URL: http://www.springerlink.com/content/v58453878n256q44/.

[4] E. Brookner and J.M. Howell, "Adaptive-Adaptive Array Processing", *Proceedings IEEE*, vol.74, pp. 604 - 604, April 1986.

[5] M. Budsabathon, Y. Hara, and S. Hara, "Optimum Beamforming for Pre-FFT OFDM Adaptive Antenna Array*," IEEE Transactions on Vehicular Technology*, vol. 53, no. 4, pp. 945 – 955, July 2004.

[6] J. Capon, "High-Resolution Frequency-Wavenumber Spectrum Analysis," *Proceedings IEEE*, vol. 57, pp.1408 – 1418, August 1969.

[7] D. J. Chapman, "Partial Adaptivity for the Large Arrays," *IEEE Transactions Antennas Propagation*, vol. AP-24, pp. 685 - 696, September 1976.

[8] Y. - F. Chen and C. - S. Wang, "Adaptive Antenna Arrays for Interference Cancellation in OFDM Communication Systems with Virtual Carriers," *IEEE Transactions on Vehicular Technology*, vol. 56, no. 4 , pp. 1837 – 1844, July 2007.

[9] J. Choi and R. W. Health, "Interpolation Based Transmit Beamforming for MIMO-OFDM with Limited Feedback," *IEEE Transactions of Signal Processing*, vol. 53, no. 11, pp. 4125 – 4135, November 2005.

[10] D. V. P. Figuieredo, M.I. Rahman, N. Marchetti, F. H. P. Fitzek, M.D. Katz, Y. Cho, and R. Prasad, "Trannsmit Diversity Vs Beamforming for Multi-User OFDM Systems," WPMC 2004.

[11] L. C. Godara, *Handbook of Antennas in Wireless Communications*, CRC Press, 2002.

[12] I. Harjula, MIMO Techniques for OFDM(A) Systems Operating in Mountainous environment, Licentiate Thesis, 91 p., 2008.

[13] S. Haykin, *Adaptive Filter Theory*, The fourth edition, Upper Saddle River, Prentice Hall, New Jersey, 920 p.,2002.

[14] M. S. Heakle, M. A. Mangoud, and S. Elnoubi, "LMS Beamforming Using Pre and Post-FFT Processing for OFDM communication Systems," 24th National Radio Science Conference, pp. 1 – 7, 2007.

[15] J. Heiskala and J. Terry, "OFDM for wireless LANs: A theoretical and practical guide," Sams, Indiana, 315 p., 2002.

[16] P. W. Howells, "Intermediate Frequency Sidelobe Canceller," Technical Report, U.S. Patent 3202990, May, 1959.

[17] *IEEE Standard Definitions of Terms for Antennas*, International standard Std 145-1993, The Institute of Electrical and Electronics Engineers, Inc., 345 East 47th Street, New York, NY 10017-2394, USA, 1993.

[18] C. K. Kim, S. Choi, and Y. S. Cho, "Adaptive Beamforming Algorithm for an OFDM System", IEEE 49th Vehicular Technology Conference, vol. 1, pp. 484 – 488, May 1999.

[19] C. K. Kim, K. Lee, and Y. S. Cho, "Adaptive Beamforming Algorithm for OFDM Systems with Antenna Arrays," *IEEE Transanctions on Consumer Electronics*, vol. 46, No. 4, pp. 1052 – 1058, November 2000.

[20] R. Kohno, "Spatial temporal Communication Theory Using Adaptive Antenna Array," IEEE Personal Communications, pp. 28 -35, 1998.

[21] M. Lei, P. Chang , H. Harada, and H. Wakana, "Adaptive Beamforming Based on Frequency-to-time Pilot Transform for OFDM," *Proceedings VTC 2004-Fall*, vol.1, pp. 285 -289, 2004.

[22] M. Lei, P. Chang , H. Harada, and H. Wakana, "A Combinational Scheme of Pre-FFT Adaptive Beamforming and Frequency-Domain Adaptive Loading for OFDM," *Proceedings VTC 2004-Fall*, vol.1, pp. 290-294, 2004.

[23] M. Lei and H. Harada, "Fast-Convergence SMI Adaptive Beamforming Based on Frequency-to-Time Pilot Transform for OFDM System," International Conference on Wireless Communications, Networking and Mobile Computing, pp.1-5, 2006.

[24] Z. Lei and F. P. S. Chin, "Post and Pre-FFT Beamforming in an OFDM system," *Proceedings VTC 2004-Spring*, vol.1, pp. 39 – 43, 2004.

[25] Y. Li and N. R. Sollenberger, "Adaptive Antenna Arrays for OFDM Systems with Cochannel Interference," *IEEE Transactions on Communications*, vol. 47, no. 2, pp. 217 – 229, February 1999.

[26] Q. Li and X. E. Lin, "Compact Feedback for MIMO-OFDM Systems over Frequency Selective Channels," *Proceedings VTC-2005-Spring*, vol.1, pp. 187 – 191, 2005.

[27] K. H. Lin, S. S. Mahmoud, and Z. M. Hussain, "Space-Time Block Coded OFDM with Adaptive Modulation and Transmitter Beamforming," Proceedings IEEE Globecom 2005, pp. 3487 – 3492, 2005.

[28] J. Litva and Titus Kwok-Yeung Lo, *Digital Beamforming in Wireless Communications*. Boston, MA: Artech House, 1996.

[29] D. R. Morgan, "Partially Adaptive Array Techniques," *IEEE Transactions Antennas Propagation*, vol. AP-26, pp. 823 – 833, November 1978.

[30] D. Parker and D. C. Zimmermann, "Phased arrays–part I: Theory and architectures," *IEEE Trans. Microwave Theory and Techniques*, vol. 50, pp. 678 – 687, March 2002.

[31] M. S. Raju et al., "BER analysis of QAM with transmit diversity in Rayleigh fading channels", *IEEE GLOBECOM '03*, pp. 641-645, Dec. 2003.

[32] Y. Sigen and R. S. Blum, "Optimized signalling for MIMO interference systems with feed back," *IEEE Transactions on Signal Processing*, vol. 51, no. 11, pp. 2839 – 2848, November 2003.

[33] B. V. Veen and K. M. Buckley "Beamforming: A versatile approach to spatial filtering," *IEEE ASSP Magazine*, vol. 5, pp. 4–24, Apr. 1988.

[34] V. Venkataraman, R. E. Gagley, and J.J. Shynk, "Adaptive Beamforming for Interference Rejection in an OFDM system," Conference Record of the Thirty-Seventh Asilomar Conference on Signals, Systems, and Computers, vol. 1, pp. 507 – 511, 2003.

[35] V. Venkataraman and J.J. Shynk, "Adaptive Interference Suppression in Multiuser OFDM," *IEEE 60th Vehicular Technology Conference*, pp. 655 – 659, 2004.

[36] F. W. Vook and K. L. Baum, "Adaptive Antennas for OFDM," *48th IEEE Vehicular Technology Conference 1998*, vol. 1, pp. 606 – 610, May 1998.

[37] J. Yang and Y. G. Li, "Low Complexity OFDM MIMO System Based on Channel Correlations", *Proceedings IEEE Globecom 2003*, vol. 1, pp. 591-595, 2003.

[38] S.- J. Yu and J.-H. Lee, "Adaptive Array Beamforming Based on an Efficient Technique," *IEEE Transactions on Antennas and Propagation*, vol. 44, pp. 1094 – 1101, August 1996.

[39] G. Zeng, F. A. Cassara, and P. Voltz, "Probability of Error for MB-OFDM System in the Presence of Multi-path Fading and Multi-User Interference", The 9th International Conference on Advanced Communication Technology, vol. 3, pp. 2079 – 2084, 2007.

[40] URL of EUWB consortium: http://www.euwb.eu

[41] H. Matsuoka and H. Shoki, "Comparison of pre-FFT and post-FFT processing adaptive arrays for OFDM systems in the presence of co-channel interference," in Proc. IEEE Personal, Indoor, and Mobile Radio Communications, 2003, pp. 1603-1607.

[42] L. Tuan et al., "A new RLS-based adaptive beamforming algorithm for smart antennas applied to an OFDM system," International Conference on Microwave and Millimeter Wave Technology, 2002, pp. 672-675.

[43] L.-Y. Fan, C. He, and X.-L. Che, "Pre-FFT adaptive beamformer based on RLS for OFDM systems," International Symposium on Antennas and Propagation Society, 2005, pp. 291-294.

[44] M. Chiani et al., "Definition of system concepts, requirements and application scenarios," EUWB deliverable D3.3.1, 2008.

[45] M. Jiang and L. Hanzo, "Multiuser MIMO-OFDM for next generation wireless systems," Proc. IEEE, vol. 95, no. 7, 2007, pp. 1430-1469.

[46] T. Kaiser and F. Zheng, Ultra Wideband Systems with MIMO, John Wiley & Sons, Ltd, 2010.

[47] H. Nguyen, Z. Zhao, F. Zheng and T. Kaiser, "On the MSI mitigation for MIMO UWB time reversal systems" ICUWB 2009, Vancouver, September 2009.

[48] T.K. Nguyen, H. Nguyen, F. Zheng and T. Kaiser, "Spatial correlation in the broadcast MU-MIMO UWB system using a pre-equalizer and Time Reversal pre-filter", Signal Processing and Communication Systems (ICSPCS), December 2010.

[49] G. Dimic and N. D. Sidiropoulos. On downlink beamforming with greedy user selection: Performance analysis and a simple new algorithm. IEEE Trans. Signal Process., 53:3857{3868, 2005.

[50] Marcin Filo, et al., "Cognitive Pilot Channel: Enabler for Radio Systems Coexistence," in Proc. CogART 2009.

[51] "Technical requirements for UWB DAA (detect and avoid) devices to ensure the protection of radiolocation in the bands 3.1 - 3.4 GHz and 8.5 - 9 GHz and BWA terminals in the band 3.4 - 4.2 GHz," ECC Report 120, June, 2008.

[52] URL of EUWB consortium: http://www.euwb.eu

Acknowledgement

The EUWB consortium would like to acknowledge the support of the European Commission partly funding the EUWB project under Grant Agreement FP7-ICT-215669 [52].